

1 **The transition from basement-involved thick-skinned to detachment thin-skinned**  
2 **tectonics in the Basque-Pyrenees: The Burgalesa Platform and vicinities.**

3 Eloi Carola<sup>1\*</sup>, Josep Anton Muñoz<sup>1</sup>, Stefano Tavani<sup>2</sup>, Eduard Roca<sup>1</sup>

4 <sup>1</sup>*GEOMODELS Research Institute, Departament de Geodinàmica i Geofísica,*  
5 *Universitat de Barcelona. C/ Martí Franquès s/n. 08028 Barcelona, Spain*

6 <sup>2</sup> *Dipartimento di Scienze della Terra. Università Federico II, Napoli. Italy.*

7  
8 \* Corresponding author: Eloi Carola.  
9 e.carola@ub.edu; eloicarola@gmail.com  
10 Universitat de Barcelona, Facultat de Geologia.  
11 C/ Martí Franquès s/n  
12 08028 Barcelona  
13 Tel.: +34 934034028  
14

15 **Bullets:**

16 - Determination of the transition from thick-skinned to thin-skinned in the Burgalesa  
17 Platform of the Basque-Pyrenees.

18 - New interpretation model for the Burgalesa Platform with thick-skinned tectonics at  
19 the western boundary and thin-skinned tectonics at the eastern one.

20 - Thickness distribution of the Upper Triassic salt allowed the detachment of the  
21 Mesozoic succession.

22  
23 **Keywords:** Thick-skinned; Thin-skinned; Inversion Tectonics; Basque-Pyrenees;  
24 Cantabrian Mountains; Burgalesa Platform.

25

26 ***Abstract***

27 Interpretation of seismic data at the margins of the Burgalesa Platform in the Basque-  
28 Cantabrian Pyrenees has allowed proposition of a new structural model that combines  
29 different modes of deformation during oblique tectonic inversion, conditioned by the  
30 distribution of Triassic salts. Deformation was decoupled by the presence of the salt  
31 horizon between basement-involved thrusts inverting formerly Triassic and Late  
32 Jurassic-Early Cretaceous extensional faults and a detached thrust system involving the  
33 Upper Triassic to Neogene sedimentary package. Such different styles of deformation  
34 were not only stacked vertically above and below the salt, but most importantly, they  
35 change from one to the other along strike across the transversal edges of the Triassic  
36 salts. The Burgalesa Platform detached thrust system was confined between the  
37 basement-involved structures of the Cantabrian Mountains westward and the NW tip of  
38 the Iberian basement-involved structures (San Pedro) southward. This together with the  
39 obliquity between the Pyrenean contractional shortening direction and the strike of the  
40 previous extensional faults, mostly at the late stages of deformation, determined the  
41 strike-slip reactivation of the basement-involved inverted faults and the lateral extrusion  
42 of the Burgalesa Platform detached Mesozoic successions above the salt toward the SE  
43 to form a prominent thrust salient oblique to the main Pyrenean trend. The proposed  
44 model combines thick-skinned with thin-skinned structural styles during oblique  
45 tectonic inversion and is consistent with the surface data, including the fracture system,  
46 the available subsurface data and the mechanical stratigraphy.

47 ***1 Introduction***

48 Structural style of orogenic systems depends on many factors such as crustal  
49 rheology, inherited structure or distribution of weak horizons (Ellis *et al.*, 1998;

50 Beaumont *et al.*, 2000; Bug and Greya, 2005; Butler *et al.*, 2006; James and Huismans,  
51 2012). Positive inversion tectonics, understood as the contractional reactivation of an  
52 extensional fault, has been documented since the 1980's in sedimentary basins using  
53 seismic data (e.g. Badley *et al.*, 1989; Chapman, 1989), field studies (e.g. Schröder,  
54 1987; Butler, 1989) and analogical modelling (e.g. Koopman *et al.*, 1987; McClay,  
55 1989). During the inversion and with the progressive incorporation of the basin into the  
56 fold and thrust belt, several geological features must be taken into account. Among  
57 others: i) the position of inherited extensional faults causing weak points within the  
58 crust and acting these as preferential deformational paths (e.g. Coward, 1994;  
59 Holdsworth, 2004; Sepher and Cosgrove, 2005; Carrera *et al.*, 2006; Mouthereau and  
60 Lacombe, 2006, Amilibia *et al.*, 2008, among others); ii) the rheology of materials and  
61 the presence of weak layers promoting the partition of deformation and controlling the  
62 evolution during inversion or the decoupling between the cover and the basement (e.g.  
63 Davis and Engelder, 1985, Bassi G. 1995; Steward *et al.*, 1997; Steward and Argent,  
64 2000); iii) the variation in stratigraphic thickness or lateral changes in facies inside the  
65 basins, due to differential subsidence, fault activity, salt mobilization or erosion  
66 controlling the spacing and distribution of main faults as well as the position of lateral  
67 structures and its propagation in space (e.g. Davis and Engelder 1985; Jaumé and Lillie,  
68 1988; Calassou *et al.*, 1993; Boyer, 1995; Mitra, 1997; Corrado *et al.*, 1998; Macedo  
69 and Marshak, 1999; Fischer and Jackson, 1999; Soto *et al.*, 2002; Spratt *et al.*, 2004;  
70 Marshak, 2004; Pfiffner, 2006). All these parameters result in two different styles of  
71 deformation during the evolution of the thrust belt. Thick-skinned tectonics, in which  
72 the basement is involved such as the inner parts of some orogens like the Alps, the  
73 Pyrenees or the Andes contrasting with the thin-skinned tectonics in which the cover is  
74 detached from the basement such as the external parts of the Pyrenees or the Zagros

75 among others. Additionally, some orogens present along-strike or along-time variation  
76 in the style of deformation (Hill *et al.*, 2002; Mazzoli *et al.*, 2008).

77         These two styles of deformation are present in the Basque Pyrenees and the  
78 Cantabrian Mountains of the Pyrenees. The first, with thin-skinned tectonics with the  
79 Mesozoic cover detached from the basement at the Upper Triassic salt layer. The  
80 second, with thick-skinned tectonics with the basement involved within the structures  
81 (Muñoz, 1992, 2002; Alonso *et al.*, 1996, Pulgar *et al.*, 1999; Vergés *et al.*, 2002;  
82 Gallastegui, 2000; Roca *et al.*, 2011). The Burgalesa Platform is the area where the  
83 along-strike transition between the two styles occurs. Both thin-skinned and thick-  
84 skinned tectonic models have been proposed in order to explain the evolution of the area  
85 either with surface geology or subsurface data thus explaining the surface geology  
86 (Hernaiz, 1994; Hernaiz *et al.*, 1994; Malagón *et al.*, 1994; Rodríguez-Cañas *et al.*,  
87 1994; Serrano *et al.*, 1994; Espina *et al.*, 1996; Espina, 1997; Pulgar *et al.*, 1999;  
88 Gallastegui, 2000; Tavani *et al.*, 2011; Quintana, 2012). The aim of this work is in one  
89 hand, to integrate the surface and subsurface data with the observations and constraints  
90 reported by other authors in order to propose a new evolution model for the Burgalesa  
91 Platform. This model contains the transition between the two styles of deformation  
92 present along-strike of the studied area. On the other hand, to better characterise the  
93 configuration of the extensional basin that controlled the contractional deformation  
94 during the Pyrenean Orogeny and the implication that it had.

## 95 ***2 Geological setting***

96         The structural evolution of the doubly-vergent Pyrenean Orogen was controlled  
97 by the inversion of Lower Cretaceous extensional basins (Beaumont *et al.*, 2000;  
98 Jammes *et al.*, 2014). The extensional event related to the opening of the North Atlantic  
99 and the Bay of Biscay during Late Jurassic-Early Cretaceous resulted in the

100 development of intracontinental basins at the rift margins, the exhumation of continental  
101 mantle at the last stages of rifting, and the spreading of oceanic crust at the western Bay  
102 of Biscay ridge (Roca *et al.*, 2011). This event allowed the local deposition of more than  
103 10 km of syn-rift sediments overlying the Jurassic carbonates and the stretched and  
104 thinned continental crust (e.g. Le Pichon and Sibuet, 1971; Montadert *et al.*, 1979;  
105 García de Cortázar and Pujalte, 1982; Pujalte, 1982; Mathieu, 1986; Ziegler, 1987;  
106 García-Mondéjar *et al.*, 1996; Bois *et al.*, 1997; Pedreira *et al.*, 2007; Ruiz, 2007; Ferrer  
107 *et al.*, 2008; Jammes *et al.*, 2009, Roca *et al.*, 2011). The convergence between the  
108 Eurasian and the Iberian plates during Late Cretaceous-Cenozoic produced the  
109 subduction of Iberia towards the north, with the subsequent inversion of the inherited  
110 Mesozoic basins (e.g. Le Pichon and Sibuet, 1971; Muñoz, 1992, 2002; Alonso *et al.*,  
111 1996; Vergés and García-Senz, 2001). The along strike structural changes of the  
112 Pyrenean orogen resulted from the inversion of a segmented rift system at the northern  
113 Iberian margin (Roca *et al.*, 2011). Thus, the Cantabrian Mountains, the Basque-  
114 Pyrenees and the Pyrenees s.s. are distinct structural domains of the Pyrenean orogen  
115 bounded by transfer faults inherited from the previous Early Cretaceous extensional  
116 system (Fig. 1A).

117         The Cantabrian Mountains, at the western part of the Pyrenean orogen (Fig. 1A  
118 and B), are constituted by Paleozoic rocks deformed during both the Variscan Orogeny  
119 (Pérez-Estaún *et al.*, 1991) and the Pyrenean Orogeny, as well as by the Permian,  
120 Triassic and Late Jurassic-Early Cretaceous extensional events. Pyrenean contractional  
121 deformation caused the reactivation of the Variscan faults and the tightening and  
122 steepening of previously developed folds (Pérez-Estaún *et al.*, 1988; Alonso *et al.*,  
123 1996; Pulgar *et al.*, 1999; Alonso *et al.*, 2009). Most of the contractional deformation  
124 has been accommodated into the northern retro-wedge along the Cantabrian margin. In

125 the southern part (pro-wedge) the thrust system involves the Variscan basement and  
126 displaced the Cantabrian Mountains towards the south over the Duero foreland basin  
127 (Álvarez-Marrón *et al.*, 1996; Pulgar *et al.*, 1997; Gallastegui, 2000; Gallastegui *et al.*,  
128 2002; Pedreira, *et al.*, 2003; Pedreira *et al.*, 2007; Roca *et al.*, 2011; Martín-González  
129 and Heredia, 2011, among others). The thrust front mostly corresponds to a fault  
130 propagation fold with its related frontal thrust only outcropping in some areas (Fig. 1A  
131 and B). As a result, the Duero basin shows a major syncline geometry.

132 Further east the Basque-Pyrenees (Fig. 1A and C) resulted from the inversion of  
133 the W-E striking Upper Jurassic-Lower Cretaceous Basque-Cantabrian Basin during the  
134 Pyrenean deformation. This is one of the basins that were developed at the southern  
135 passive margin of the Bay of Biscay. The Basque-Pyrenees are displaced southward  
136 more than 15 km over the Ebro Foreland Basin by means of a south-directed low-angle  
137 thrust detached into the Upper Triassic evaporites (Martínez-Torres, 1993; Carola *et al.*,  
138 2013). The frontal structure (Sierra de Cantabria Frontal Thrust) and associated folds  
139 present a north-facing concave shape in map view where in the central parts they strike  
140 almost W-E whereas, at the edges they progressively rotate to a more WSW-ENE and  
141 NW-SE orientation in the east and west respectively (Fig. 1A).

142 In continuation with the Cantabrian Mountains and to the southwest of the  
143 Basque Pyrenees there is a distinct structural domain known as Burgalesa Platform (Fig.  
144 1A). It consists of a moderately deformed succession of Triassic to Upper Cretaceous  
145 sediments with some preserved syn-tectonic Miocene continental rocks. The Burgalesa  
146 Platform shows a thrust salient with a prominent bend at its eastern edge where  
147 structures change the trend from WNW-ESE to NE-SW (Fig. 1A).

148           There is not a consensus as far as the tectonic style and the structural evolution  
149 of the Burgalesa Platform are concerned. Different structural models have been  
150 proposed during the last decades, among them the most distinct ones are: i) low-angle  
151 thin-skinned; ii) low-angle thick-skinned, and iii) transpressive high-angle thick-skinned  
152 (Fig. 1D). In the thin-skinned model, the Jurassic-Cretaceous succession is detached  
153 from the Variscan basement into the Triassic evaporites and transported at least 10 km  
154 southward (Hernaiz, 1994; Hernaiz *et al.*, 1994; Malagón *et al.*, 1994; Rodríguez-Cañas  
155 *et al.*, 1994; Serrano *et al.*, 1994). The low-angle thick-skinned model is based on the  
156 existence of a basement-involved low-angle thrust below the Mesozoic succession, in  
157 continuation with the floor thrust of the thrust system deforming the Cantabrian  
158 Mountains (Espina *et al.*, 1996; Alonso *et al.*, 1996; Espina, 1997; Pulgar *et al.*, 1999;  
159 Gallastegui, 2000; Alonso *et al.*, 2007; Quintana, 2012). Finally, in the third model the  
160 contractional structures are transpressive elements related with high-angle and deeply-  
161 rooted right-lateral strike-slip faults, such as the Ubierna fault (Tavani *et al.*, 2011). The  
162 implication of this third model is that the Burgalesa Platform Domain would represent  
163 an uplifted area of the deformed Duero foreland.

164           These contrasting models are based on different data sets, mostly from surface  
165 geology, that at least partially support the proposed structural evolution for each model.  
166 A question arises about which of these models is the most consistent with all the  
167 available data in the area (surface and subsurface) and compatible with other  
168 considerations such as the inherited structures, the mechanical stratigraphy of the rocks  
169 involved or the kinematics of the area. This work brings together subsurface and surface  
170 data in order to discuss a new model. Any proposed structural model would have to  
171 consider the Late Jurassic-Early Cretaceous extensional faults that deformed the area as  
172 well as the presence of a thick layer of Triassic salts as drilled by numerous wells.

### 173 **3 Tectonostratigraphic units of the Burgalesa Platform**

174 The stratigraphic succession of the study area can be divided into several units,  
175 which are associated to the different tectonics events that took place from Triassic to  
176 Cenozoic times (Fig. 2).

177 The Paleozoic succession is made up of Ordovician quartzites and phyllites , Devonian  
178 ferruginous sandstones, Carboniferous limestones and Permian clays. The Lower to  
179 Middle Triassic sediments are constituted by conglomerates and sandstones of the  
180 Buntsandstein facies and dolostones of the Muschelkalk facies, which are associated to  
181 the rifting stage that produced the breakup of Pangea (Van Veen, 1965; Wagner *et al.*,  
182 1971; García-Mondéjar *et al.*, 1986; Alonso, 1987). All the pre-Upper Triassic  
183 succession is referred as basement throughout the paper.

184 Above, the Upper Triassic Keuper facies consists of salt, anhydrite, gypsum and shales  
185 with sub-volcanic basic intrusions. This unit is the most important detachment level. Its  
186 ability to flow under the right conditions is the responsible of its irregular distribution as  
187 evidenced by the amount of diapirs present in the study area (i.e. Aguilar (Serrano and  
188 Martínez del Olmo, 2004), Poza de la Sal (Hempel, 1967; Quintà *et al.*, 2012), Salinas  
189 del Rosío (Hernáiz and Solé, 2000), among others). This unit is widespread all along the  
190 Pyrenees, although it is absent in significant areas (i.e. eastern Pyrenees, aragonese  
191 western Pyrenees) as well as in the Cantabrian Mountains.

192 After the Triassic extensional event, a quiescence stage took place during the Jurassic.  
193 This period of time is characterised by the development of a carbonate ramp, mainly  
194 limestones and dolostones with interbedded evaporites at the lower parts of the unit.  
195 Whereas, deep marine hemipelagic sediments with limestones, marls and shales

196 characterise the upper portions of this unit (Pujalte *et al.*, 1988; Robles *et al.*, 1989,  
197 2004; Quesada *et al.*, 1991, 1993, 2005; Aurell *et al.*, 2003).

198 The second and main extensional event is related to the opening of the North Atlantic  
199 and the Bay of Biscay during the Late Jurassic to Early Cretaceous. The stratigraphic  
200 record of this period in the Burgalesa Platform is characterised by fluvio-deltaic  
201 siliciclastic sandstones that locally reach more than 4 km (Pujalte, 1981, 1982; Pujalte *et*  
202 *al.*, 1996, 2004; Hernández *et al.*, 1999). Forced folding of the Jurassic succession and  
203 salt mobilization took place during this extensional event (Tavani *et al.*, 2013).

204 The upper Albian-Upper Cretaceous succession is made up of conglomerates and  
205 sandstones at the base and limestones and marls at the top post-dating the Early  
206 Cretaceous extension. It is associated to a gradual deepening of the succession passing  
207 from continental to marine environment during several transgressive events (Aguilar,  
208 1971; Ramirez del Pozo, 1971; Portero, 1979).

209 The Cenozoic syn-orogenic sediments are mainly constituted by conglomerates,  
210 sandstones and red clays. The pebbles and cobbles are mainly from the Upper  
211 Cretaceous limestones and dolostones (Portero *et al.*, 1979). This unit is restricted to the  
212 border of the study area (i.e. Ebro and Duero foreland basins) and also in the Bureba  
213 Sub-basin and Villarcayo syncline (Fig. 3).

#### 214 ***4. Structure of The Burgalesa Platform***

215 The internal structure of the Burgalesa Platform is dominated at surface by wide and  
216 gentle folds with very shallow dips affecting the Upper Cretaceous limestones. Most of  
217 the contractional structures are located between the thrust front and the Ubierna fault  
218 where they define a narrow belt of folds and related thrusts (Folded Band, Fig. 3). North  
219 of the Ubierna fault there is a structural continuity between the Cantabrian Mountains

220 and the Burgalesa Platform at surface as evidenced by a continuous tilted panel towards  
221 the ESE of Triassic to Upper Cretaceous rocks overlying the Variscan basement (Fig.  
222 3). To the north, there is also an apparent structural continuity with the Basque  
223 Pyrenees, although a series of anticlines and faults connect the structures in the Ebro  
224 reservoir area with the Sierra de Cantabria Frontal Thrust, thus representing the northern  
225 edge of the Burgalesa Platform (Fig. 3). The SE part of the Burgalesa Platform is  
226 characterised by NE-SW trending folds (Hontomín flexure, Rojas), along which salt  
227 structures occur (Poza de la Sal, Hontomín and Rojas domes). These folds developed  
228 during the sedimentation of the Miocene fluvial deposits that finally covered them,  
229 masking the relationships between the NE-SW structures, the Ebro Basin and the Sierra  
230 de Cantabria frontal thrust. The upper and younger Miocene conglomerates define a re-  
231 entrant in map view between the Sierra de Cantabria thrust front and the Burgalesa  
232 Platform (Fig. 3). At surface the significance of such re-entrant cannot be deciphered,  
233 mostly if it is only the result of the unconformable disposition of the Miocene  
234 conglomerates over the NE-SW structures that would connect with the Sierra de  
235 Cantabria thrust or if, alternatively, represents a structural re-entrant of the Ebro Basin  
236 between the Basque Pyrenees and the Burgalesa Platform. The solution given to this  
237 uncertainty has a strong impact on the structure and the deduced structural evolution of  
238 the Burgalesa Platform and can only be resolved by subsurface data as will be discussed  
239 later on. The Miocene syn- to post-tectonic sediments of the Duero Basin also mask the  
240 frontal structure of the Burgalesa Platform and also the available subsurface data is  
241 crucial for its proper understanding.

242 Here below the main structural features of the Burgalesa Platform and its relationships  
243 with the surrounding units will be discussed in detail taken advantage of the available  
244 seismic sections and well data acquired in the area for hydrocarbon exploration.

#### 245 **4.1. Interpretation of the seismic and well data**

246 A seismic profile across the Cantabrian Mountains thrust front, west of the Burgalesa  
247 Platform, shows the thick-skinned structural style of this unit as well as its relationships  
248 with the Duero foreland basin (Fig. 4). The floor of the Paleogene-Neogene Duero  
249 Basin is characterised by a continuous and constant thickness succession of the upper  
250 Albian-Upper Cretaceous post-rift sediments (sandstones of the Utrillas Fm. and  
251 limestones) unconformably overlying the Paleozoic basement rocks (Gallastegui, 2000).  
252 These sediments crop out at surface in the hangingwall of the frontal thrust with  
253 subvertical to overturned northward steeply dipping beds structurally above the  
254 Devonian rocks. The bedding attitude of the Cretaceous sediments in the hangingwall  
255 together with the location of the south-dipping reflections of the equivalent succession  
256 in the seismic section define the frontal syncline of a fault propagation fold and  
257 demonstrate the reduced displacement of the frontal thrust in the subsurface. Moreover,  
258 this thrust does not reach the surface as the younger syn-orogenic Neogene  
259 conglomerates, adjacent to the thrust front, show a progressive unconformity above the  
260 Paleogene vertical conglomerates that overlie the Upper Cretaceous limestones (Fig. 4).  
261 Thrusts and related folds also affect the basement and the Upper Cretaceous sediments  
262 in the Duero foreland basin. Their displacement caused growth geometries in the  
263 younger Neogene clastic sediments (Fig. 4).

264 An E-W seismic profile across the eastward tilted panel of Triassic to Lower Cretaceous  
265 stratigraphic units illustrates the transition between the eastern edge of the Cantabrian  
266 Mountains and the Burgalesa Platform Domain (Fig. 5). In this section, the east-dipping  
267 panel of continuous and strong reflections attributed to the Jurassic and to the Lower  
268 Cretaceous terminates in a syncline. Below the Mesozoic tilted panel, a set of west-  
269 dipping reflections has been imaged into the chaotic seismic facies of the basement

270 between 3,5 and 2 TWT seconds (Fig. 5). It has been considered as a continuous  
271 seismic event, which merges with the axial surface of the above described syncline at  
272 the bottom of the Mesozoic succession, and interpreted as a thrust involving the  
273 basement of the Cantabrian Mountains, climbing up section laterally into the Upper  
274 Triassic evaporites of the Burgalesa Platform. This structure has the same structural  
275 position as the frontal anticline of the Cantabrian Mountains in the hangingwall of the  
276 floor thrust of the basement-involved thrust system, but differently with respect to the  
277 Duero basin the thrust was not emergent as it detached into the Triassic salts. Thus, east  
278 of the syncline, the Mesozoic succession of the Burgalesa Platform has been detached  
279 above the basement.

280 Detachment of the Burgalesa Platform from the basement can also be deduced from the  
281 interpretation of the seismic lines located further east. Two seismic lines across the  
282 Huidobro anticline, at the northern edge of the Burgalesa Platform, reveal a significant  
283 structural relief of the Jurassic succession above a continuous set of gently northward-  
284 dipping reflectors interpreted as the top of the basement (Fig. 6). The identification of  
285 the different packages of reflectors relies not only on their seismic facies, but also on the  
286 data supplied by the Tejón Profundo-1 well in the S-84-110 seismic line (Fig. 6A). The  
287 Tejón Profundo-1 well, drilled in the Huidobro anticline, encountered a repetition of the  
288 Mesozoic succession at 1700 meters below the surface. In addition, the register shows a  
289 thick salt succession (1200 m) underneath the lower Jurassic without reaching the  
290 bottom of the Keuper at the end of the well (3800 m.b.s.). The most puzzling geometry  
291 revealed by these seismic lines and the well is the mismatch of the positive structural  
292 relief when comparing the top of the Jurassic succession and the bottom of the Upper  
293 Cretaceous sediments. The amplitude of the anticline related to the back-thrust that  
294 duplicated the Jurassic and Lower Cretaceous beds decreases significantly in the Upper

295 Cretaceous succession. Moreover, there are no evidence of growth sediments into this  
296 succession and, most importantly, these sediments where deposited before the onset of  
297 the Pyrenean convergence. The Lower Cretaceous succession presents a thickening  
298 towards the south being this succession almost twice thicker than the succession in the  
299 Huidobro anticline where, in its turn, the Upper Triassic is significantly thicker. These  
300 relationships reveal salt withdrawal and salt inflation (Fig. 6).

301 East of the Huidobro anticline, the northern edge of the Burgalesa Platform is  
302 characterised by the NW-SE trending Villalta anticline (Fig. 3). An oblique seismic  
303 section across it shows its structure at depth (Fig. 7). The Upper Triassic to Jurassic  
304 succession of the NE limb of the anticline is involved into a hangingwall ramp above a  
305 flat-lying thrust that would be the eastward continuation of the back-thrust imaged in  
306 the Huidobro anticline by N-S trending seismic profiles (Figs. 6 and 7). The flat-lying  
307 reflections in the footwall would be in continuation with the Lower Cretaceous to  
308 Triassic succession drilled by the Tejón Profundo-1 well underneath the Huidobro back-  
309 thrust. These sediments are involved in the Poza de la Sal antiform and the related salt  
310 structure (Figs. 3 and 7). In the central sector of the seismic profile the shallower  
311 Mesozoic-Cenozoic reflectors appear folded in contrast with the flat-lying reflectors  
312 underneath at 2 TWT seconds. In the easternmost part, the Cenozoic and Upper  
313 Cretaceous sediments of the foreland basin have been imaged by more than 2 TWT  
314 seconds of strong, continuous and parallel reflections. They present similar signature  
315 and seismic facies as shown by seismic profiles in the Duero Basin further to the west.  
316 The lower reflections are characterised by an upper continuous and high amplitude set  
317 of reflectors above a semitransparent unit and a lowermost unit of continuous  
318 reflections lying above the acoustic basement. These 3 seismic units correspond to the  
319 Upper Cretaceous succession of the Duero Basin, which has been drilled by numerous

320 exploration wells (compare Figs. 9 and 4, Gallastegui, 2000). The Cenozoic sediments  
321 progressively cover the allochthonous Mesozoic units towards the west, although the sole  
322 thrust truncates the lower ones. West of the thrust front the reflectors corresponding to  
323 the autochthonous Upper Cretaceous are difficult to follow westward underneath the  
324 sole thrust. They are truncated at the western edge of the profile by a strong west-  
325 dipping reflection that has been interpreted as a footwall ramp of the sole thrust.

326 The SE edge of the Burgalesa Platform corresponds to the NE-SW trending Rojas  
327 anticline (Fig. 3). A seismic section across the northern continuation of the Rojas  
328 anticline below the Miocene sediments shows a frontal thrust and a related anticline  
329 similar to and in continuation with the frontal structure described in the previous  
330 seismic section (Figs. 7 and 8). As a result, the geometry of the thrust front at the SE  
331 edge of the Burgalesa Platform would show a significant thrust salient, concave to the  
332 WNW, if the younger Miocene sediments would be removed. The seismic section of  
333 Figure 8 shows the relationships between the Burgalesa Platform and the Ebro foreland  
334 basin at its westernmost reentrant between the Burgalesa Platform and the Basque  
335 Pyrenees (Fig. 3). In the eastern portion of the section, the foreland is imaged as a layer  
336 cake succession of strong and continuous reflectors of the Cenozoic and Upper  
337 Cretaceous sediments. The thrust truncates the lower part of the Cenozoic succession  
338 and its related anticline shows growing relationships with the middle to upper part of  
339 the Cenozoic foreland basin sediments corresponding to the Early to Middle Miocene.  
340 The western part of the seismic section is dominated by a wedge of Lower Cretaceous  
341 sediments sandwiched between lower subhorizontal reflectors, Jurassic in age, and an  
342 upper east-dipping panel of Upper Cretaceous sediments. The Lower Cretaceous wedge  
343 thins eastward and the reflectors onlap onto the Jurassic succession

344 A seismic section located northeastward of the Burgalesa Platform and crossing the  
345 Sierra de Cantabria Frontal Thrust shows the thin-skinned tectonic style of deformation  
346 in this part of the orogen (Fig. 9). The Jurassic to Cenozoic succession has been  
347 detached above the Upper Triassic salts and thrust on top of the flat-lying Cretaceous  
348 to Cenozoic sediments of the Ebro foreland basin in continuation with the foreland  
349 described in previous seismic sections. The foreland is imaged as a layer cake parallel  
350 succession at all directions as shown by the W-E and S-N sections in which no  
351 deformation is visible. In this area, more than 1.5 seconds TWT thick succession of  
352 strong and continuous reflections alternate with weak reflections attributed to the  
353 Cenozoic foreland basin infill. Additionally in the Rioja 1 well, located towards the  
354 south-east in the Ebro foreland basin, more than 3 km of Cenozoic succession was  
355 testified (Lanaja, 1987). Below the Cenozoic, strong and continuous reflections  
356 characteristic of the Upper Cretaceous seismic facies and the upper Albian overlie the  
357 basement. In the hangingwall, the Lower Cretaceous succession experiences a  
358 thickening towards the north. The northern part of the section is characterised by the  
359 Villarcayo syncline filled with Cenozoic sediments and where the Trespaderne-1 well is  
360 located.

#### 361 **4.2. Interpretation of the structure: integration of surface and subsurface data**

362 Three south-north and one northwest-southeast cross-sections integrating the  
363 surface geology and the subsurface data, allow to determine on one hand, the transition  
364 between the two styles of deformation and on the other hand, the structural significance  
365 of the Burgalesa Platform with respect to the Pyrenean Orogen (Fig. 10).

366 The westernmost S-N cross-section is characterised by basement involved structures,  
367 outcropping in the northern sector, whereas, detached structures occur in the southern

368 part (I-I' in figure 10). The transition between the two domains occurs southwards of the  
369 Golobar fault where the depocenter of the syn-extensional sediments is located. South  
370 of this transition, the syn-rift succession progressively thins contrasting with the  
371 Triassic salts that thickens towards the Ubierna Fault. The wells drilled in the  
372 hangingwall of this structure (i.e. Basconcillos-1 and Abar-1) testify both, a strongly  
373 incomplete Jurassic succession and the duplication of the syn-rift sediments below the  
374 Jurassic. The interpretation for this structure is that of a small back-thrust, rooted into  
375 the Triassic salt layer cutting a previously developed extensional fault that produced the  
376 partial omission of the Jurassic and the thickening of the Triassic salt. Southwards, in  
377 the folded band, both the Jurassic and the syn-rift successions are reduced. The thrust  
378 system climbs up southwards being this part of the Burgalesa Platform riding over the  
379 Duero Foreland Basin and also over the north-directed and basement involved San  
380 Pedro structure.

381 Similar to the previous one, the middle S-N cross-section shows the involvement of the  
382 basement in the northern sector and the detachment of the Mesozoic in the southern one  
383 (II-II' in figure 10). The transition between the two styles takes place northwards of the  
384 Lower Cretaceous depocenter where the Cadialso-1 well drilled more than 3 km of syn-  
385 rift sediments. The northern area is characterised by the presence of a salt wall in the  
386 Ebro area in which the Cabañas-1 well testifies the omission of the Jurassic succession.  
387 To the north, the surface geology allows to constrain the thrust that uplifts the Jurassic  
388 succession outcropping westwards of the trace of the cross-section (Fig. 3). South of the  
389 depocenter the syn-rift succession thins until it reaches the Ayoluengo salt-cored  
390 structure, where the wells drilled a thickness of *ca.* 1000 meters of Lower Cretaceous  
391 rocks. The southern sector of the Burgalesa Platform is characterised by the thrusting  
392 over the Duero Foreland Basin and by a thinning of both, the Jurassic and syn-rift

393 successions. The southernmost part of the cross-section is where the San Pedro wells  
394 are located, constraining the presence of this structure at depth.

395 The easternmost S-N cross-section here presented shows the prolongation of the Ebro  
396 reservoir salt wall at the northern sector (III-III' in figure 10). In this area, the Navajo-1  
397 well testifies a thin syn-rift succession directly overlying the Triassic salts, with the  
398 omission of the Jurassic rocks. The well drilled more than 2000 meters of Triassic salts  
399 and reached the top of the basement at 3900 meters below the surface (m.b.s.).  
400 Contrasting with this, the adjacent Arco Iris-1 and Manzanedo-1 wells drilled all the  
401 Cretaceous and the Jurassic successions. These data suggest that the Navajo antiform  
402 resulted from the squeezing of a salt wall related with an Early Cretaceous extensional  
403 fault in the hangingwall of a basement involved thrust.

404 In the Huidobro area, as stated before, the back-thrust duplicates the succession as  
405 testified by both, the Tejón Profundo-1 well and the seismic line (Fig. 6). However, a  
406 problem arises when comparing the amount of shortening observed in the pre-rift  
407 Jurassic horizons and the one observed in the Upper Cretaceous beds (Fig. 10). Part of  
408 this mismatch in the amount of shortening can be the result of the obliquity between the  
409 cross-section and the thrust transport direction. Nevertheless, this would not explain the  
410 observed difference. In addition, this would not also explain the differences in structural  
411 relief between the deeper structural levels and the shallower ones (Fig. 6). Such  
412 difference in the structural relief results into the unconformity at the bottom of the post-  
413 rift upper Albian-Upper Cretaceous sediments and the erosional truncation geometry of  
414 the syn-rift horizons below the unconformity, mostly visible in the southern limb of the  
415 Huidobro anticline (see details in the seismic lines of Fig. 6). Differences in the  
416 structural relief can be partially explained by salt inflation during rifting. The southern  
417 limb of the salt body drilled by the Tejón Profundo-1 well will be the locus of the back-

418 thrust during the subsequent contractional deformation at Paleogen-Neogene times  
419 (Hernaiz et al., 1994; Malagón et al., 1994). The other explanation for the observed  
420 structural relationships, and mostly the unconformity observed at the bottom of the post-  
421 rift succession, would be that part of the observed contractional deformation is pre  
422 upper Albian, and thus linked with the extensional system as part of a toe system. The  
423 Early Cretaceous extensional basins were transported to the N-NE and detached above  
424 the Triassic salts. The structural relief created by salt structures during the extensional  
425 deformation, such as salt walls and diapirs along the northern edge of the Burgalesa  
426 Platform would have controlled the geometry and location of contractional structures in  
427 the northern part of Burgalesa Platform. The possible existence of salt welds basinward  
428 the salt structures would have enhanced the contractional reactivation of the flanks of  
429 the salt structures facing the rift margin. The existence of Early Cretaceous  
430 contractional features were already cited by Serrano *et al.* (1994), although not  
431 documented, these contractional structures are commonly related with the distal parts of  
432 extensional systems (Peel *et al.*, 1995; Rowan *et al.*, 1999; Rowan *et al.*, 2004; Lacoste  
433 *et al.*, 2012; Cartwright *et al.*, 2012, among others). Southwards, the thrust system  
434 climbs up section and overrides the Duero Foreland Basin. In this part, a narrow  
435 corridor between the Burgalesa Platform and the San Pedro Structure is present.

436 Finally, the NW-SE section illustrates the transition between thick-skinned and thin-  
437 skinned styles of deformation in the NW-SE direction (IV-IV' in figure 10). In the  
438 north-western part, the basement is involved in the thrust system and as a consequence  
439 the Mesozoic sequence is uplifted and tilted towards the SE as described in figure 5. In  
440 this portion, the Coto-1 well drilled a thin Triassic salt succession before the top of the  
441 basement at *ca.* 3000 m.b.s. Eastward, the Mesozoic succession is detached into the  
442 Triassic salts as stated before (Fig. 5). The hangingwall cutoff of the basement coincides

443 with the depocentre of the syn-rift sediments, as does in sections I and II, where Triassic  
444 salts were thin, either depositionally or by welding during the salt withdrawal towards  
445 the margins of the basins. The syn-rift succession thins above the inflated salt, reaching  
446 less than 1000 meters in the Huidobro-2 well. From this sector to the Villalta-1 well, the  
447 oblique to the transport view of the back-thrust is the main structural feature as  
448 described in figure 7. In this section, the differences in the structural relief between the  
449 Upper Cretaceous beds and the Jurassic ones in relation with the thrust that duplicates  
450 the pre-rift succession, as well as the lack of evidence of a major back-thrust at surface,  
451 reinforces the Early Cretaceous age for part of this structure. The south-eastern edge of  
452 the Burgalesa Platform is characterised by the perpendicular view of the salt-cored  
453 Rojas structure and the frontal thrust system climbing over the Ebro Foreland Basin.

454 Determining the main succession boundaries by integrating all the subsurface data  
455 allows to characterise the distribution pattern of the main depocenters and thinned areas  
456 (Fig. 11). The distribution of the Triassic salt layer has two main trends in the Burgalesa  
457 Platform. On the one hand, the NE-SW orientation present in the Ayoluengo and Rojas  
458 area where in this latter case a total thickness of 1400 meters was drilled by the well  
459 Rojas NE-1. On the other hand, the WNW-ESE orientation present along the northern  
460 block of the Ubierna Fault System, where the wells Abar-1 with 1000 meters, the Pino-  
461 1 with 300 meters or the Montorio-1 with 450 meters of salt is present, and along the  
462 Villalta anticline in where the Tejón Profundo-1 well drilled more than 1200 meters of  
463 Upper Triassic salts. All these thicknesses are minimum values because the wells did  
464 not drilled the whole Upper Triassic reaching the succession located below. In contrast,  
465 the Coto-1 well only drilled 100 meters of Triassic salts and reached the basement at  
466 more than 4000 meters below the surface. In contraposition, the Lower Cretaceous  
467 distribution can be summarised in an opposite manner of the Upper Triassic salt

468 distribution. The thinned areas corresponds to the thickened salt areas such as the  
469 northern block of the Ubierna fault in the Ayoluengo structure and in the Villalta areas.  
470 The thickened syn-rift area is located to the NW where the salt accumulation is  
471 minimum. Even though in this area the Lower Cretaceous is outcropping and the total  
472 thickness cannot be precisely determined, a total thickness of almost 3000 meters is  
473 registered by the Coto-1 well. The thinned south-eastern area is associated with the  
474 boundary of the extensional basin during the Cretaceous as demonstrated by the seismic  
475 line described in figure 8 where the syn-rift drastically reduces its thickness and also  
476 how onlap onto the Jurassic. The onlap stated before, extends in a broad band almost  
477 parallel to the Ubierna fault trace displaying a southwards direction of migration (Fig.  
478 12A). The map view trace of the onlaps has a roughly WNW-ESE orientation with a  
479 bend in the middle where it attains a more NW-SE orientation thus similar as the  
480 Ubierna fault. A S-N seismic section crossing the southern limit of the Burgalesa  
481 Platform shows a southern sector, in which thrusts deform the whole Mesozoic  
482 successions and a northern sector where cover deformation is almost absent (Fig. 12B).  
483 The southern area corresponds to the Folded Band located southwards of the Burgalesa  
484 Platform and the seismic facies do not allow to interpret the Mesozoic successions.  
485 Whereas, the northern area is characterised by north-dipping pre-rift panel, a  
486 sedimentary wedge constituted by syn-rift successions and an almost horizontal post-rift  
487 succession eroding the one located immediately below (Fig. 12B). Within the  
488 sedimentary wedge, the sedimentary geometry observable onlaps both the pre-rift and  
489 the syn-rift successions with a southwards direction of migration extending from the  
490 northern limit of the seismic and ending close to the Ubierna fault.

## 491 *5 Discussion*

492 The data and structural interpretations herein included demonstrate the strong  
493 decoupling of the Mesozoic successions from the basement rocks located below the  
494 Upper Triassic salts in the Burgalesa Platform and, in general, in the Basque Pyrenees.  
495 Decoupling occurred during both the Late Jurassic-Early Cretaceous extensional  
496 deformation and the subsequent tectonic inversion and fold and thrust development at  
497 Paleogene-Neogene times.

498 The scarcity of extensional faults bounding the main depocenters of the syn-rift  
499 sequences, the onlap geometries of the syn-rift beds onto the Jurassic carbonates lying  
500 above the Triassic salts and all the observed salt structures that developed during the  
501 extensional deformation suggest that salt decoupled deformation above and below. Of  
502 particular relevance are the contractional structures described in the northern part of  
503 the Burgalesa Platform (Fig. 6). They involve a few kilometres of shortening and  
504 demonstrate decoupling and a significant detachment of the cover of the Burgalesa  
505 Platform to the N-NE during thin-skinned extensional deformation.

506 Extensional faults affecting the cover mostly emerged at the rift margins, at present  
507 inverted along the thrust front southward the Ubierna fault system. These faults marked  
508 a sharp transition in the stratigraphic record. Thus, at the rift shoulders, at present the  
509 Duero and Ebro foreland basins, the Mesozoic pre-rift sequences are not preserved, the  
510 syn-rift sediments were not deposited and the upper Albian post-rift sequences  
511 unconformably overlie the basement rocks. This stratigraphy is constant in the foreland  
512 all along the thrust front including in the Bureba re-entrant at the NE edge of the  
513 Burgalesa Platform (Fig. 7 and 9). In the hangingwall of the marginal extensional  
514 detachment a gap in the pre-rift Jurassic should be expected to account for the onlap  
515 geometries in the Burgalesa Platform, as observed in the most frontal preserved thrust  
516 imbricates. Such Jurassic gaps related with the extensional detachment have also been

517 observed and described further east in the Basque Pyrenees and in the Bay of Biscay  
518 (Jammes *et al.*, 2009; Rowan, 2014).

519 The extensional faults affecting the Upper Triassic salts as well as the cover in the  
520 Burgalesa Platform produced the migration of salt. The sedimentation of the syn-rift  
521 successions accentuated the salt mobilisation (Vendeville and Jackson, 1992; Hudec and  
522 Jackson, 2007, among others). At the end of the extensional deformation, the salt  
523 thickness distribution pattern was characterised by two areas of major accumulation  
524 surrounded by areas where the thickness of the salt layer was depleted and even welded  
525 (Fig. 11). The WNW-ESE orientation was associated to inherited Late Permian-Triassic  
526 extensional structures reactivated during the Late Jurassic-Early Cretaceous extensional  
527 event and the NE-SW orientation associated to newly develop extensional faults  
528 (Tavani and Muñoz, 2012 and Tavani *et al.*, 2013). The Ubierna, Huidobro and Navajo  
529 areas are characteristic of the first orientation whereas, the Rojas area at the easternmost  
530 boundary is characteristic of the second orientation. As a consequence, this salt  
531 distribution has a strong impact during the inversion of the basin. This characteristic is  
532 well known and the configuration of the former basin, the mechanical stratigraphy and  
533 the thickness and the spatial distribution of the ductile levels can determine differential  
534 advance of the thrust system towards the foreland basin with respect to areas where this  
535 level is absent or strongly reduced (Jaumé and Lille, Davis and Engelder, 1985;  
536 Bahroudi and Koyi, 2003; Luján *et al.*, 2003; Sepehr *et al.*, 06; Vidal *et al.*, 2009;  
537 among others).

538 Extensional faults thinning the basement below the Triassic salt should be expected to  
539 occur northward the emergent marginal extensional fault system. The Ubierna fault and  
540 related salt structure would be located above a basement-involved high-angle  
541 extensional fault offsetting the base of the salt. However, the salt was thick enough to

542 allow decoupling during northward-directed detachment and developed drape folds  
543 above the basement step. A northward displacement of more than 10 km above the  
544 extensional detachment is necessary to explain the width of the observed onlap  
545 geometries north of the Ubierna structure as shown in figure 12. This would be also  
546 consistent with the described syn-extensional contractional features northwards and the  
547 distribution of the syn-rift depocenters.

548 The spatial and thickness distribution of the Triassic pre-rift salt was dependent on the  
549 geometry of the Triassic extensional faults, which controlled the topography at the time  
550 of evaporite deposition during the late to sag phase of the Triassic rifting. In the western  
551 part of the Basque Pyrenees Triassic extensional faults (Ubierna, Golobar and Rumaceo  
552 faults among others) were arranged in a left stepped way. Rely ramps connecting the  
553 extensional faults were characterised by eastward dipping panels, some of them  
554 probably breached as suggested by Espina (1997), and defined an approximately north  
555 trending western edge of the Triassic salts.

556 Decoupling did not occur at the western edge of the Burgalesa Platform because of the  
557 absence of the Upper Triassic salts, either by no deposition or by erosion during the  
558 Late Jurassic-Early Cretaceous rifting. The western edge of the Triassic salts coincides  
559 with the transition from the thin-skinned tectonic style of the frontal part of the Basque  
560 Pyrenees and the Burgalesa Platform eastward to the thick-skinned tectonic style of the  
561 Cantabrian Mountains westward. There, coupling of the basement and cover during the  
562 Pyrenean deformation resulted in an increase of the structural relief and the eastward  
563 plunge of the structures at the eastern termination of the Cantabrian Mountains (Alonso  
564 *et al.*, 1996; Espina, 1997; Tavani *et al.*, 2013). Recent AFT and ZHe  
565 thermochronological data by Fillon (2012) along a cross-section in the eastern part of  
566 the Cantabrian Mountains yield a Late Eocene age for the onset of the exhumation of

567 the basement involved during the inversion of the Cabuérniga and Rumaceo faults.  
568 Exhumation continued southward into the hangingwall of the Golobar fault at  
569 Oligocene times. A youngest Early Miocene exhumation age was acquired in the  
570 basement rocks in the hangingwall at the western termination of the Ubierna fault once  
571 uplift ended further north. Southward migration of basement exhumation is consistent  
572 with a forward propagating thrust system involving both basement and cover rocks and  
573 inverting the previously developed Triassic and Late Jurassic-Early Cretaceous  
574 extensional faults (Alonso *et al.*, 1996; Fillon, 2012). Moreover, the old exhumation  
575 ages (Jurassic to Paleocene) recorded in Cretaceous and Stephanian rocks along the  
576 thrust front (Fillon, 2012) demonstrate the limited amount of uplift and related  
577 displacement of the frontal thrust in agreement with the fault-propagation fold model  
578 suggested by Alonso *et al.* (1996).

579 As stated before, this N-S western boundary of the Burgalesa Platform has an eastward  
580 plunge, for this reason, the map view allows to project the surface geology towards the  
581 east and to extrapolate the subsurface geology downwards as shown by Tavani *et al.*  
582 (2013). However, in the light of the surface and subsurface data provided in this work,  
583 we must clarify that this down-plunge projection cannot be extrapolated eastward the  
584 transition between the two styles of deformation. This is because more to the east the  
585 Upper Triassic salt layer detaches the Mesozoic succession from the basement (Fig. 5).  
586 This disharmony between the cover and the basement is denoted by the surface geology  
587 in the area east of Aguilar where the cover structures are not reflected into the basement  
588 and with the amount of contractional and salt structures aligned along this N-S  
589 boundary such as the Aguilar, the Reinoso or the Pas structures from south to north  
590 (Espina, 1997, Fig. 3). The only structure that partially truncates the décollement level  
591 at the western Burgalesa Platform is the Golobar fault (Fig. 3). This would be in

592 agreement with the right-lateral strike slip reactivation of the formerly inverted Golobar  
593 extensional fault during the last stages of deformation (Tavani *et al.*, 2011), coeval with  
594 the progression of deformation into the basement below the Burgalesa Platform (Fig. 5  
595 and 10). Uplift and exhumation of the hangingwall of the Golobar fault during tectonic  
596 inversion occurred at Oligocene times (Fillon, 2012) and the right-lateral reactivation  
597 with reduced uplift would be younger.

598 Integration of all the observations, constraints and data presented in this work together  
599 with the data reported by several authors in the last years, requires a new model to  
600 explain the structural evolution of the Burgalesa Platform. The proposed model is a  
601 combination of thin-skinned and thick-skinned modes of deformation. Decoupling and  
602 related thin-skinned structures have been controlled by the initial distribution of Triassic  
603 salts. On the contrary, basement-involved structures have mostly determined by the  
604 reactivation of extensional faults. Oblique inversion tectonics played also a significant  
605 role. The increase of the obliquity between the strike of the faults and the shortening  
606 direction as the Pyrenean deformation progressed would have favoured strike-slip  
607 reactivation, both in the cover and in the basement, and lateral extrusion of the  
608 Burgalesa Platform (Tavani *et al.*, 2011; Quintà and Tavani, 2012).

609 The thick-skinned domain is characterised by the WNW-ESE to W-E basement-  
610 involved thrust structures of the Cantabrian Mountains (Alonso *et al.*, 1996;  
611 Gallastegui, 2000; Tavani *et al.*, 2013) and the Duero foreland basin (Fig. 4,  
612 Gallastegui, 2000). In addition, in this area, Tavani *et al.* (2011) reported the  
613 transpressive reactivation of outcropping faults (i.e. Ubierna, Golobar, Rumaceo). The  
614 thin-skinned domain spans eastwards of the basement cutoff along most of the entire  
615 Burgalesa Platform and also in the Basque-Pyrenees. This domain is characterised by

616 the detachment and south-eastwards extrusion of the Burgalesa Platform as previously  
617 pointed out by Rodríguez Cañas *et al.* (1994) and Tavani *et al.* (2011).

618 The moderate deformation of the Upper Cretaceous sediments, with predominant  
619 subhorizontal beds at a roughly similar height, and the strong deformation along the  
620 southern and eastern edges of the Burgalesa Platform (Folded Band and Rojas structure  
621 respectively) are consistent with a fold and thrust belt detached on salt, being its edges  
622 determined by the abrupt termination of the Triassic salts in the hangingwall of previous  
623 extensional faults. The interpretation of the seismic data in the Bureba re-entrant of the  
624 Ebro foreland basin at the northern edge of the Rojas structure is crucial for the thin-  
625 skinned interpretation of the Burgalesa Platform (Fig. 3). The continuity of the seismic  
626 stratigraphy of the Bureba re-entrant with the Ebro and Duero basins, the salient  
627 geometry of the Rojas structure and the attitude of the different tectonostratigraphic  
628 packages there demonstrate detachment and thrusting of the Mesozoic successions of  
629 the Burgalesa Platform above the Duero-Ebro basins (Figs. 8 and 9). Thrust transport  
630 direction would be to the SE as suggested by the geometry of the Rojas salient  
631 (Rodríguez Cañas *et al.*, 1994). The geometry of the Bureba re-entrant prevents any  
632 attempt to connect the NE-SW trending Rojas structure with the Sierra de Cantabria  
633 frontal thrust with a continuous NE trend (Fig. 3) as it is done in many published  
634 structural sketches of the area. Moreover, a NW-SE trending thrust connecting the Rojas  
635 and Poza de la Sal is required to account for the stratigraphic differences between the  
636 foreland and the Burgalesa Platform, as observed in seismic sections (Fig. 7 and Fig. 8).  
637 The resulting geometry of the SE edge of the Burgalesa Platform can be hardly  
638 explained by a thick-skinned structural style. It would require the tectonic inversion of  
639 three different extensional faults: the Ubierna fault southward, the Rojas one eastward  
640 and a northern SW dipping one. There are evidence for the first two, but not for the

641 latter. In addition, inversion of such fault system involving the basement would require  
642 vertical tectonics and piston-like deformation mode. This is not compatible with surface  
643 data neither with the geometries observed in seismic lines.

644 The attitude of the autochthonous Upper Cretaceous top cutoff line, located in the  
645 footwall of the sole thrust, gives an idea of the allochthony of the Burgalesa Platform.  
646 To know the position of such line, the NW tip of the Bureba re-entrant (Figs. 3 and 9)  
647 can be connected with the northernmost outcropping Upper Cretaceous folded  
648 sediments of the Duero foreland basin that are located to the south of the eastern  
649 Cantabrian Mountains basement rocks tip (Figs. 3 and 13). Such a line has an almost W-  
650 E trend in continuation with the equivalent cutoff line in the footwall of the Sierra de  
651 Cantabria frontal thrust (Fig. 13). The quality of the available seismic data does not  
652 allow to fully constrain the position of this line at depth below the Burgalesa Platform.

653 As shown in many tectonic settings (i.e. contractional, extensional or strike-slip) when a  
654 ductile level like salt or even shales is present the deformation is decoupled between the  
655 basement and the cover (Jaumé and Lille, 1988; Peel *et al.*, 1995; Coward and Stewart,  
656 1995; Rowan *et al.*, 1999; Withjack and Callaway, 2000; Durand-Riard *et al.*, 2013;  
657 among others). This fact would make difficult to explain that in the study area, where a  
658 thick salt succession is present, the deformation was not decoupled across this layer thus  
659 resulting in a thick-skinned deformation.

660 With the proposed model, the amount of overlap between the allochthonous Mesozoic  
661 succession of the Burgalesa Platform and the autochthonous Mesozoic of the Ebro and  
662 Duero Foreland increase towards the southeast. This is denoted in figure 13 where the  
663 actual thrust front limit of the Burgalesa Platform and the limit of the Upper Cretaceous  
664 Autochthonous Footwall Cutoff (UCAFC) are overlapped. As shown for the south-

665 eastern part of the cross-section IV-IV' (Fig. 10) and at the seismic section (Fig. 7) the  
666 amount of south-east displacement of the Burgalesa Platform with respect to the  
667 autochthonous is almost 15 km being this value close to the right-lateral displacement  
668 for the Ubierna Fault System pointed by Tavani *et al.* (2011). This south-east  
669 displacement is also in agreement with the Upper Cretaceous fracture pattern of the  
670 Burgalesa Platform (Quintà and Tavani, 2012).

671 This proposed model reflects the actual configuration of the studied area but it resulted  
672 from the partitioning of deformation through time. For such reason, the evolution is  
673 subdivided into three main stages each one characterised by a different kinematic of the  
674 structures. During the early stages of deformation, the north-directed basement-involved  
675 thrusts deforming the San Pedro structure were developed. At this time, the Burgalesa  
676 Platform was southward displaced thus reactivating and inverting the former  
677 extensional faults detaching the whole Mesozoic succession above the Upper Triassic  
678 salts. At the end of this deformational period, the San Pedro structure resulted in a NW-  
679 SE orientation in map view (Fig. 13). As deformation continued, the Burgalesa Platform  
680 was displaced towards the south until it overrode the San Pedro structure (Fig. 3). At  
681 this point, and may be because this latter structure acted as a backstop for the southward  
682 displacement of the Burgalesa Platform, the WNW-ESE Ubierna fault was reactivated  
683 in a right-lateral sense thus forcing the Burgalesa Platform to extrude towards the south-  
684 east overriding the Ebro Foreland Basin. During the last stages of deformation, the  
685 reactivation of basement structures deformed the Duero foreland and also the western  
686 Burgalesa Platform. Regarding to the reactivation of the Golobar fault, it would be in  
687 agreement with the deformation of the inner parts of the fold and thrust belt in order to  
688 preserve the taper (Davis *et al.*, 1983; Dahlen, 1990; Boyer, 1995, among others). In  
689 addition, the oblique inversion of basement structures located below the detached

690 Mesozoic succession could be expected during the late stages of deformation as it  
691 progressed south-eastwards.

692 Even though the similarities in structural style between the San Pedro structure and the  
693 structures deforming the Duero foreland basin south of the Cantabrian Mountain front  
694 they were disconnected and are related to different thrust belts during the Cenozoic  
695 contractional stage. This asseveration is supported by the foreland deformation map  
696 pattern and by the relative timing between the different structures of both sectors  
697 partially constrained by the relative age of growth sediments and the exhumation ages  
698 of the eastern Cantabrian Mountains. On the one hand, the NW-SE San Pedro structure  
699 would be related to the Iberian Range. The north-directed basement-involved thrust of  
700 the San Pedro structure and the decrease of deformation westwards of this structure  
701 would be in agreement with the attribution of this structure as the westward  
702 continuation of the northern wedge of the Iberian Range in which the same  
703 characteristics are described (Álvaro *et al.*, 1979; Guimerà, 1984; Guimerà *et al.*, 1995;  
704 Salas *et al.*, 2001; Guimerà *et al.*, 2004). In addition, the obliquity between the NW-SE  
705 San Pedro structure and the WNW-ESE Burgalesa Platform together with the relative  
706 timing, being the San Pedro structure overrode by the Burgalesa Platform, also supports  
707 the disconnection between the two structural units. On the other hand, the southern  
708 deformation of the Cantabrian Mountain would be related to the Pyrenees instead of the  
709 Iberian Range. The eastwards decrease of deformation of the W-E orientated south-  
710 directed basement-involved structures described in the foreland together with the  
711 relative timing between the structures and the thermochronological ages of the  
712 Cantabrian Mountains are in agreement with the southward propagation of deformation  
713 of the Pyrenees.

714 **6 Conclusions**

715           The data presented in this study allowed to propose a new evolution model for  
716 the Burgalesa Platform which fully match with all the surface, subsurface and  
717 mechanical stratigraphic constraints. It supports the interpretation of the Burgalesa  
718 Platform as a result of the interference between thick- and thin-skinned styles of  
719 deformation, both in time and space, during the Cenozoic contractional stage. The  
720 western part or the Burgalesa Platform, close to the Cantabrian Mountains, is  
721 characterised by south-directed basement-involved structures whereas, the eastern part  
722 is characterised by thrusts detached at the Upper Triassic salts overriding the foreland  
723 basin. These differences are related to the distribution of the Upper Triassic salt layer,  
724 resulted from the Triassic and Late Jurassic-Early Cretaceous extensional events, that  
725 controlled the deformation during the Pyrenean Orogeny. The boundary that divides the  
726 two styles of deformation connects the easternmost deformation of Cantabrian  
727 Mountains in the Duero foreland basin with the western area of the Basque Pyrenees.  
728 This boundary crosses the Burgalesa Platform between the Golobar and Ayoluengo  
729 areas with a SW-NE orientation.

730           The confined location of the Burgalesa Platform with respect to the Cantabrian  
731 Mountains and the San Pedro structure together with the obliquity between the strike of  
732 extensional faults and the shortening direction of the Pyrenean Orogeny conditioned the  
733 evolution of the Burgalesa Platform. During the early stages of deformation, the  
734 southward displacement of the whole Basque-Cantabrian Pyrenees was coeval with the  
735 northward-directed San Pedro structure. As deformation continued, the right-lateral  
736 reactivation of the Ubierna Fault System, due to the backstop produced by the San  
737 Pedro Structure, resulted in the more than 15 km of south-east lateral extrusion of the  
738 Burgalesa Platform over the Ebro Foreland Basin. At the last stage of contraction

739 reactivation of basement thrusts at the western sector deformed the Duero Foreland  
740 Basin as well as the Burgalesa Platform.

#### 741 **7 Acknowledgments**

742 This work was carried out under the financial support of INTECTOSAL (CGL2010-  
743 21968-C02- 01/BTE) and CIUDEN (FBG305657) projects and also the “Grup de  
744 Recerca de Geodinàmica i Anàlisi de Conques” (2009SGR-1198). The Instituto  
745 Geológico y Minero de España (I.G.M.E.) is thanked for providing seismic sections. We  
746 also thank Seismic Micro-Technology and Midland Valley which generously provided  
747 Kingdom Suite and Move software.

#### 748 **8 References**

- 749 Aguilar, M.J. 1971. Correlaciones por ciclos de aporte en el Albense de la Cuenca  
750 Cantábrica. *Acta Geológica Hispánica* **6**, 92-96.
- 751 Alonso, J.L. 1987. Estructura y evolución tectonoestratigráfica de la región del Manto  
752 del Esla (Zona Cantábrica NW de España). Tesis Doctoral. Universidad de Oviedo.  
753 276pp.
- 754 Alonso, J.L., Pulgar, J.A., García-Ramos, J.C., Barba, P., 1996. Tertiary Basins and  
755 Alpine Tectonics in the Cantabrian Mountains. In: Friend, P.F., Dabrio, C.J., (eds.).  
756 Tertiary basins of Spain: The stratigraphic record of crustal kinematics. Cambridge,  
757 Cambridge University Press, 214-227.
- 758 Alonso, J.L., Pulgar, J.A., Pedreira, D. 2007. Relieve de la Cordillera Cantábrica.  
759 *Enseñanza de las Ciencias de la Tierra*, **15.2**, 151-163.
- 760 Alonso, J.L., Marcos, A., Suárez, A. 2009. Paleogeographic inversion resulting from  
761 large out of sequence breaching thrusts: The León Fault (Cantabrian Zone, NW  
762 Iberia). A new picture of the external Variscan Thrust Belt in the Ibero-Armorian  
763 Arc. *Geologica acta*, **7**, 451-473.
- 764 Álvarez-Marrón, J., A. Pérez-Estaún, J.J. Danñobeitia, J.A. Pulgar, R. Martínez Catalán,  
765 A. Marcos, F. Bastida, P. Ayarza Arribas, J. Aller, A. Gallart, F. Gonzalez-Lodeiro,  
766 E. Banda, M.C. Comas and D. Córdoba. 1996. Seismic structure of the northern  
767 continental margin of Spain from ESCIN deep seismic profiles. *Tectonophysics*. vol.  
768 264, pp. 153-174.

- 769 Álvaro, M., Capote, R., Vegas, R. 1979. Un modelo de evolución geotectónica para la  
770 cadena Celtibérica. *Acta Geologica Hispanica*, **14**, 172-181.
- 771 Amilibia, A., Sàbat, F., McClay, K.R., Muñoz, J.A., Roca, E., Chong, C. 2008. The role  
772 of inherited tectono-sedimentary architecture in the development of central Andean  
773 mountain belt: Insights from the Cordillera de Domeyko. *Journal of Structural  
774 Geology*. **30**, 1520-1539.
- 775 Aurell, M., Robles, S., Bádenas, B., Rosales, I., Quesada, S., Meléndez, G., García-  
776 Ramos, J.C. 2003. Transgressive-regressive cycles and Jurassic paleogeography of  
777 northeast Iberia. *Sedimentary Geology*, **162**, 239-271. doi:10.1016/S0037-  
778 0738(03)00154-4.
- 779 Badley, M.E., Price, J-D., Backshall, L.C. 1989. Inversion, reactivated faults and related  
780 structures: seismic examples from the southern North Sea. In: Inversion tectonics  
781 Cooper, M.A. and Williams, G.D. (eds). *Geological Society Spececial Publications*.  
782 **44**, 201-219.
- 783 Bahroudi, A. and Koyi, H.A., 2003. Effect of spatial distribution of Hormuz salt on  
784 deformation style in the Zagros fold and thrust belt: an analogue modelling approach.  
785 *Journal of the Geological Society of London* **160**, pp. 719-733. doi: 10.1144/0016-  
786 764902-135.
- 787 Barnolas, A., Pujalte, V., 2004. La Cordillera Pirenaica. In: Vera, J.A. (Ed.), *Geología  
788 de España*. Madrid, SGE-IGME, 233–343.
- 789 Bassi, G. 1995. Relative importance of strain rate and rheology for the mode of  
790 continental extension. *International Journal Geophysics*. **122**, 195-210.
- 791 Beaumont, C., Muñoz, J.A., Hamilton J., Fullsack, P., 2000. Factors controlling the  
792 Alpine evolution of the central Pyrenees inferred from a comparison of observations  
793 and geodynamical models. *Journal of Geophysical Research*, **105**, 8121-8145.
- 794 Bois, C.; Pinet, B., Gariel, O. 1997. The sedimentary cover along the ECORS Bay of  
795 Biscay deep seismic reflection profile. A comparison between the Parentis basin and  
796 other European rifts and basins. *Mémoires de la Société Géologique de France*, **171**,  
797 143-165.
- 798 Boyer, S. 1995. Sedimentary basin taper as a factor controlling the geometry and  
799 advance of thrust belts. *American Journal of Science*. **295**, 1220-1254.
- 800 Bug, J.P., Greya, T.V. 2005. The role of viscous heating in Barrovian metamorphism of  
801 collisional orogens: thermomechanical models and application to the Lepontine  
802 Dome in the Central Alps. *Journal Metamorphic Geology*, **23**, 75-95.
- 803 Butler, R.W.H., Tavarnelli, E., Grasso, M. 2006. Structural inheritance in mountain  
804 belts: an Alpine–Apennine perspective, *Journal of Structural Geology* **28**, pp. 1893-  
805 1908. doi:10.1016/j.jsg.2006.09.006.

- 806 Butler, R.W.H. 1989. The influence of pre-existing basin structure on thrust system  
807 evolution in the Western Alps. In: Inversion tectonics Cooper, M.A. and Williams,  
808 G.D. (eds). *Geological Society Spececial Publications*. **44**, 105-122.
- 809 Calassou, S., Larroque, C., Malavielle, J. 1993. Transfer zones of deformation in thrust  
810 wedges: An experimental study. *Tectonophysics*, **221**, 325-344.
- 811 Carola, E.; Tavani, S.; Ferrer, O.; Granado, P.; Quintà, A.; Butillé, M.; Muñoz, J.A.  
812 2013. Along-strike extrusion at the transition between thin- and thick-skinned  
813 domains in the Pyrenean Orogen (northern Spain). In *Thick-skin-dominated*  
814 *Orogens: From initial inversion to full accretion*. Nemcok, M.; Mora, A.R.;  
815 Cosgrove, J.W. (eds). *Geological Society of London Special Publications* **377**,  
816 DOI:10.1144/SP377.3.
- 817 Carrera, N., Muñoz, J.A., Sàbat, F., Mon, R., Roca, E. 2006. The role of inversion  
818 tectonics in the structure of the Cordillera Oriental (NW Argentinean Andes).  
819 *Journal of Structural Geology*, **28**, 1921-1932.
- 820 Cartwright, J., Jackson, M., Dooley, T., Higgins, S. 2012. Strain partitioning in gravity-  
821 driven shortening of a thick, multilayered evaporite sequence. In: *Salt Tectonics,*  
822 *Sediments and Prospectivity*. Alsop, G.I., Archer, S.G., Hartley, A.J., Grant, N.T.,  
823 Hodgkinson, R. (eds). *Geological Society of London Special Publications* **363**, 449-  
824 470.
- 825 Chapman, T.J. 1989. The Permian to Cretaceous structural evolution of the Western  
826 Approaches Basin (Melville sub-basin), UK. In: Inversion tectonics Cooper, M.A.  
827 and Williams, G.D. (eds). *Geological Society Spececial Publications*. **44**, 177-200.
- 828 Corrado, S., Bucci, D., Naso, G., Faccenna, C. 1998. Influence of paleogeography on  
829 thrust system geometries: an analogue modelling approach from the Abruzzi-Molise  
830 (Italy) case history. *Tectonophysics*, **296**, 437-453.
- 831 Coward, M.P., 1994. Inversion Tectonics. In: Hancock, P.L. (Ed.), *Continental*  
832 *Deformation*, Pergamon Oxford, 289-304.
- 833 Coward, M.P., Stewart, S. 1995. Salt-induced structures in the Mesozoic-Tertiary cover  
834 of the southern North Sea U.K. In: M.P.A. Jackson, D.G. Roberts, and S. Snelson  
835 (eds). *Salt tectonics: a global perspective*. *AAPG Memoir*, **65**, 229-250.
- 836 Dahlen, F.A. 1990. Critical taper model of fold-and-thrust belts and accretionary  
837 wedges. *Annual reviews earth and planetary science*. **18**, 55-99.
- 838 Davis, D., Suppe, J., Dahlen, F.A. 1983. Mechanics of Fold-and-Thrust belts and  
839 accretionary wedges. *Journal of Geophysical Research*, **88**, 1153-1172.
- 840 Davis, D.M., Engelder, T. 1985. The role of salt in fold-and-thrust belts. *Tectonophysics*  
841 119, 67-88.

- 842 Durand-Riard, P., Shaw, J.H., Plesch, A., Lufadeju, G. Enabling 3D geomechanical  
843 restoration of strike- and oblique-slip faults using geological constraints, with  
844 applications to the deep-water Niger Delta. *Journal of Structural Geology*, **48**, 33-44.  
845 DOI: 10.1016/j.jsg.2012.12.2009.
- 846 Ellis, S., Beaumont, C., Jamieson, R.A., Quinlan, G. 1998. Continental collision  
847 including a weak zone: the vise model and its application to the Newfoundland  
848 Appalachians. *Canadian Journal of Earth Science*, **35**, 1323-1346.
- 849 Espina, R.G. 1997. La estructura y evolución tectonoestratigráfica del borde occidental  
850 de la Cuenca Vasco-Cantábrica (Cordillera Cantábrica, NO de España) Ph.D. Thesis,  
851 University of Oviedo. 230pp.
- 852 Espina, R.G., De Vicente, G., Muñoz Martín, A. 1996. Análisi poblacional de fallas  
853 alpinas en el borde occidental de la Cuenca Vasco-Cantábrica (Cordillera  
854 Cantábrica, NO de España). *Geogaceta*. **20** 936-938.
- 855 Ferrer, O., E. Roca, B. Benjumea, J. A. Muñoz, N. Ellouz, and MARCONI Team. 2008.  
856 The deep seismic reflection MARCONI-3 profile: role of extensional Mesozoic  
857 structure during the Pyrenean contractional deformation at the eastern part of the Bay  
858 of Biscay. *Marine and Petroleum Geology*, **25(8)**, 714-730.  
859 doi:10.1016/j.marpetgeo.2008.06.002.
- 860 Fillon, C. 2012. Spatial and temporal variation in Cenozoic exhumation of the  
861 Pyrenean-Cantabrian mountain belt: coupling between tectonics and surface  
862 processes. PhD Thesis. Institut des Sciences de la Terre de Grenoble (ISTerre),  
863 Grenoble, France. 202p.
- 864 Fischer, M.P., Jackson, P.B., 1999. Stratigraphic controls on deformation patterns in  
865 fault-related folds: a detachment fold example from the Sierra Madre Oriental,  
866 northeast Mexico. *Journal of Structural Geology* **21**, 613-633.
- 867 Gallastegui, J. 2000. Estructura cortical de la Cordillera y Margen Continental  
868 Cantábricos: Perfiles ESCI-N. *Trabajos Geología*, **22**, 9-234.
- 869 Gallastegui, J., J. A. Pulgar, and J. Gallart. 2002. Initiation of an active margin at the  
870 North Iberian continent-ocean transition. *Tectonics*, **21(4)**, doi:  
871 10.1029/2001TC901046.
- 872 García de Cortázar, A., Pujalte, V., 1982. Litoestratigrafía y facies del grupo  
873 Cabuérniga (Malm-Valanginiense Inferior?) al S de Cantabria-NE de Palencia.  
874 *Cuadernos Geología Ibérica* **8**, 5-21.
- 875 García-Mondéjar, J., Pujalte, V., Robles, S. 1986. Características sedimentológicas  
876 secuenciales y tectoestratigráficas del Triásico de Cantabria y Norte de Palencia.  
877 *Cuadernos de Geología Ibérica*, **10**. 151-172.

- 878 García-Mondéjar, J., Agirrezabala, L.M., Aranburu, A., Fernández-Mendiola, P.A.,  
879 Gómez-Pérez, I., López-Horgue, M., Rosales, I. 1996. Aptian-Albian tectonic pattern  
880 of the Basque-Cantabrian Basin (northern Spain). *Geological Journal* **31**, 13-45.
- 881 Guimerà, J. 1984. Palaeogene evolution of deformation in the north-east Iberian  
882 Peninsula. *Geological Magazine*, **121**, 413-420.
- 883 Guimerà, J., Alonso, A., Mas, R. 1995. Inversion of an extensional-ramp basin by a  
884 newly formed thrust: The Cameros Basin (N Spain). *In*: Buchanan, J.G. and  
885 Buchanan, P.G. (eds). *Basin Inversion*. Geological Society of London Special  
886 Publications, **88**, 433-453.
- 887 Guimerà, J., Mas, R., Alonso, Á. 2004. Intraplate deformation in the NW Iberian Chain:  
888 Mesozoic extension and Tertiary contractional inversion. *Journal of the Geological*  
889 *Society of London* **161**, 291-303.
- 890 Hempel, P.M. 1967. Der diapir von Poza de la Sal (Nordspanien). *Beiheft Geologisches*  
891 *Jahrbuch* **66**, 95-126.
- 892 Hernáiz, P.P., Solé, J. 2000. Las estructuras del diapiro de Salinas del Rosío y del alto  
893 de San Pedro-Iglesias y sus implicaciones en la evolución tectónica de la transversal  
894 burgalesa de la Cordillera Vasco-cantábrica-Cuenca del Duero. *Rev. Soc. Geol.*  
895 *España* **13** 471-486.
- 896 Hernáiz, P.P., Serrano, A., Malagón, J., Rodríguez Cañas, C. 1994. Evolución  
897 estructural del margen SO de la cuenca Vasco Cantábrica. *Geogaceta*. V15. pp. 143-  
898 146.
- 899 Hernáiz, P.P. 1994. La falla de Ubierna (margen SO de la cuenca Cantábrica).  
900 *Geogaceta*. **16**. 39-42.
- 901 Hernández, J.M<sup>a</sup>., Pujalte, V., Robles, S., Martín-Closas, C. 1999. División  
902 estratigráfica genética del grupo Campóo (Malm-Cretácico Inferior, SW Cuenca  
903 Vasco-cantábrica). *Rev. Soc. Geol. España* **12** 377-396.
- 904 Hill, K.C., Kendrick, R.D., Crowhurst, P.V., Gow, P.A. 2002. Copper-gold  
905 mineralisation in New Guinea: tectonics, lineaments, thermochronology and  
906 structure. *Australian Journal of Earth Sciences*. **49**, 737-752.
- 907 Holdsworth, R.E., 2004. Weak faults, rotten cores. *Science* **303**, 181-182. doi:  
908 10.1126/science.1092491.
- 909 Hudec, M.R., Jackson, M.P.A. 2007. Terra infima: Understanding salt tectonics. *Earth*  
910 *Science reviews* **82**, 1-28. DOI: 10.1016/j.earscirev.2007.01.001.
- 911 Jammes, S., G. Manatschal, L. Lavier, and E. Masini. 2009. Tectonosedimentary  
912 evolution related to extreme crustal thinning ahead of a propagating ocean: the  
913 example of the western Pyrenees, *Tectonics*, **28**, TC4012,  
914 doi:10.1029/2008TC002406.

- 915 James, S., Huismans, R.S. 2012. Structural styles of mountain building: controls of  
916 lithospheric rheologic stratification and extensional inheritance. *Journal of*  
917 *Geophysical Research*, **117**, 1978-2012.
- 918 Jammes, S., Huismans, R.S., Muñoz, J.A. 2014. Lateral variations in structural style of  
919 mountain building: controls of rheological and rift inheritance. *Terra Nova*  
920 DOI:10.1111/ter.12087.
- 921 Jaumé, S. C., R. J. Lillie. 1988. Mechanics of the Salt Range-Potwar Plateau, Pakistan:  
922 A fold-and-thrust belt underlain by evaporites, *Tectonics*, **7**, 57- 71.
- 923 Koopman, A., Speksnijder, A., Horsfield, W.T. 1987. Sandbox model studies of  
924 inversion tectonics. *Tectonophysics*, **137**, 379-388.
- 925 Lacoste, A., Vendeville, B.C., Mourgues, R., Loncke, L., Lebacq, M. 2012.  
926 Gravitational instabilities triggered by fluid overpressure and downslope incision -  
927 Insights from analytical and analogue modelling. *Journal of Structural Geology*, **42**,  
928 151-162. DOI: 10.1016/j.jsg.2012.05.011.
- 929 Lanaja, J. M. 1987. *Contribución de la exploración petrolífera al conocimiento de la*  
930 *Geología de España*. IGME, Serv. Oubl. Min. Indust. Energ., Madrid. 465 pp.
- 931 Le Pichon, X., Sibuet, J.C., 1971. Western extension of boundary between European  
932 and Iberian plates during the Pyrenean orogeny. *Earth and Planetary Science Letters*  
933 **12**, 83-88. doi:10.1016/0012-821X(71)90058-6.
- 934 Luján, M., Storti, F., Balanyá, J.C., Crespo-Blanc, A. and Rossetti, F., 2003. Role of  
935 décollement material with different rheological properties in the structure of the  
936 Aljibe thrust imbricate (Flysch Trough, Gibraltar Arc): an analogue modelling  
937 approach. *Journal of Structural Geology* **25**, pp. 867–881. doi:10.1016/S0191-  
938 8141(02)00087-1.
- 939 Macedo, J., Marshak, S. 1999. Controls on the geometry of fold-thrust belt salients.  
940 *Geological Society of America Bulletin*, **111**, 1808-1822.
- 941 Malagón, J., Hernáiz, P.P., Rodríguez Cañas, C., Serrano. 1994. Notas sobre la  
942 inversión tectónica y aloctonia de la cuenca Vasco-Cantábrica. *Geogaceta*. **15**. 139-  
943 142.
- 944 Marshak, S., 2004. Salients, recesses, arcs, oroclines, and syntaxes: a review of ideas  
945 concerning the formation of map-view curves in fold-thrust belts. In: McClay, K.R.  
946 (Ed.), Thrust tectonics and hydrocarbon systems. *Memoir of the American*  
947 *Association of Petroleum Geologists* **82**, pp. 131-156.
- 948 Martínez-Torres, L. M. 1993. Corte balanceado de la Sierra Cantabria (cabalgamiento  
949 de la Cuenca Vasco-Cantábrica sobre la Cuenca del Ebro), *Geogaceta*, **14**, 113-115.

- 950 Martín-González, F. & Heredia, N. 2011. Complex tectonic and tectonostratigraphic  
951 evolution of an Alpine foreland basin: The western Duero Basin and the related  
952 Tertiary depressions of the NW Iberian Peninsula. *Tectonophysics* 502, 75-89.  
953 doi:10.1016/j.tecto.2010.03.002.
- 954 Mathieu, C. 1986. Histoire géologique du sous-bassin de Parentis. *Bulletin des Centres*  
955 *de Recherches Elf-Aquitaine (Production)*, **10**, 33-47.
- 956 Mazzoli, S., D'Errico, M., Allega, L., Corrado, S., Invernizzi, C., Shiner, P., Zattin, M.,  
957 2008. Tectonic burial and 'young' (b10 Ma) exhumation in the southern Apennines  
958 fold and thrust belt (Italy). *Geology* **36**, 243-246.
- 959 McClay, K.R. 1989. Analogue models of inversion tectonics. In: Inversion tectonics  
960 Cooper, M.A. and Williams, G.D. (eds). *Geological Society Special Publications*.  
961 **44**, 41-59.
- 962 Mitra, G. 1997. Evolution of salients in a fold-and-thrust belt: the effects of sedimentary  
963 basin geometry, strain distribution and critical taper. In: Sengupta, S. (Ed.) *Evolution*  
964 *of Geological Structures in Micro- to Macro-scales*, Chapman and Hall, London. 59-  
965 90.
- 966 Montadert, L., Charpal, O., Roberts, D. G., Guennoc, P., Sibuet, J. C. 1979. Northeast  
967 Atlantic passive margins: rifting and subsidence processes. *American Geophysics*  
968 *Union, Revue*, **3**, 154-186.
- 969 Mouthereau, F., Lacombe, O. 2006. Inversion of the Paleogene Chinese continental  
970 margin and thick-skinned deformation in the Western Foreland of Taiwan. *Journal of*  
971 *Structural Geology*. **28**, 1977-1993.
- 972 Muñoz, J. A. 1992. Evolution of a continental collision belt: ECORS-Pyrenees crustal  
973 balanced section, in *Thrust Tectonics*, edited by K. R. McClay, pp. 235-246,  
974 Chapman and Hall, London.
- 975 Muñoz, J. A. 2002. The Pyrenees, in *The Geology of Spain*, edited by W. Gibbons and  
976 T. Moreno, pp. 370-385. Geological Society of London, London.
- 977 Pedreira, D., J. A. Pulgar, J. Gallart, and J. Díaz. 2003. Seismic evidence of Alpine  
978 crustal thickening and wedging from the western Pyrenees to the Cantabrian  
979 Mountains (north Iberia). *Journal of Geophysical Research*, **108**(B4), doi:  
980 10.1029/2001JB001667.
- 981 Pedreira, D., Pulgar, J. A., Gallart, J., Torné, M. 2007. Three-dimensional gravity and  
982 magnetic modeling of crustal indentation and wedging in the western Pyrenees-  
983 Cantabrian Mountains, *J. Geophys. Res.*, **112**(B12405), doi: 10.1029/2007JB005021.
- 984 Peel, F., Travis, C.J., Hossack, J.R. 1995. Genetic structural provinces and salt tectonics  
985 of the Cenozoic offshore US gulf of Mexico: a preliminary analysis. In: M.P.A.

- 986 Jackson, D.G. Roberts, and S. Snelson (eds). Salt tectonics: a global perspective.  
987 *AAPG Memoir*, **65**, 153-175.
- 988 Pérez-Estaún, A., Bastida, F., Alonso, J.L., Marquinez, J., Aller, J., Álvarez-Marrón, J.,  
989 Marcos, A., Pulgar, J. 1988. A thin-skinned Tectonics Model for an arcuate fold and  
990 thrust belt: The Cantabrian Zone (Variscan Ibero-Armorican Arc). *Tectonics* **7**, 517-  
991 537.
- 992 Pérez-Estaún, A., Martínez-Catalán, J.R., Bastida, F. 1991. Crustal thickening and  
993 deformation sequence in the footwall to the suture of the Variscan belt of northwest  
994 Spain. *Tectonophysics*. **191**. 243-253. doi:10.1016/0040-1951(91)90060-6.
- 995 Pfiffner, O. A. 2006. Thick-skinned and thin-skinned styles of continental contraction.  
996 In: Mazzoli, S. and Butler, R. W. H. (eds) *Styles of Continental Contraction*.  
997 *Geological Society of America Special Paper*, **414**, 153-177. doi:  
998 10.1130/2006.2414(09).
- 999 Portero, J.M., Ramírez del Pozo, J., Aguilar, M. 1973. Mapa geológico 1:50.000, Hoja  
1000 170 (Haro). IGME.
- 1001 Pujalte, V., Robles, S., Valles, J.C. 1988. El Jurásico marino de las zonas de alto  
1002 sedimentario relativo del borde SW de la Cuenca Vasco-Cantábrica (Rebolledo de la  
1003 Torre, Palencia). In: *III Coloquio de Estratigrafía y Paleogeografía del Jurásico de*  
1004 *España. Libro guía de las excursiones*. Ciencias de la Tierra (Instituto de Estudios  
1005 Riojanos), **11**, 85-94.
- 1006 Pujalte, V., Robles, S., Hernández, J.M<sup>a</sup>. 1996. La sedimentación continental del Grupo  
1007 Campóo (Malm-Cretácico basal de Cantabria, Burgos y Palencia): testimonio de un  
1008 reajuste hidrográfico al inicio de una fase rift. *Cuad. Geol. Ibérica*, **21** 227-251.
- 1009 Pujalte, V., Robles, S., García-Ramos, J.C., Hernández, J.M. 2004. El Malm-  
1010 Barremiense no marinos de la Cordillera Cantábrica. In: Vera, J.A. (ed.) *Geología de*  
1011 *España*. SGE-IGME, Madrid, 288-291.
- 1012 Pujalte, V. 1981. Sedimentary succession and palaeoenvironments within fault-controlled  
1013 basin: the "Wealden" of the Santander area, Northern Spain. *Sedimentary Geology*  
1014 **28**, 293-325.
- 1015 Pujalte, V. 1982. La evolución paleogeográfica de la cuenca "Wealdense" de Cantabria.  
1016 *Cuadernos de Geología Ibérica*, **8** 65-83.
- 1017 Pulgar, J.A., Pérez-Estaún, A., Gallart, J., Álvarez-Marrón, J., Gallastegui, J., Alonso,  
1018 J.L. and ESCIN Group. 1997. The ESCIN-2 deep seismic reflection profile: a  
1019 traverse across the Cantabrian Mountains and adjacent Duero basin. *Revista*  
1020 *Sociedad Geológica de España*. **8**, 383-394.
- 1021 Pulgar, J. A., Alonso, J. L., Espina, R. G., Marín, J. A. 1999. La deformación alpina en  
1022 el basamento varisco de la Zona Cantábrica, *Trabajos de Geología*. **21**, 283-294.

- 1023 Quesada, S., Robles, S., Pujalte, V. 1991. Correlación secuencial y sedimentológica  
1024 entre registros de sondeos y series de superficie del Jurásico Marino de la Cuenca de  
1025 Sanander (Cantabria, Palencia y Burgos). *Geogaceta* **10**, 3-10.
- 1026 Quesada, S., Robles, S., Pujalte, V., 1993. El Jurásico Marino del margen suroccidental  
1027 de la Cuenca Vasco-Cantábrica y su relación con la exploración de hidrocarburos.  
1028 *Geogaceta* **13**, 92-96.
- 1029 Quesada, S., Robles, S., Rosales, I., 2005. Depositional architecture and transgressive–  
1030 regressive cycles within Liassic backstepping carbonate ramps in the Basque–  
1031 Cantabrian basin, northern Spain. *Journal Geological Society of London*. **162**, 531-  
1032 548.
- 1033 Quintà, A., Tavani, S., Roca, E. 2012. Fracture pattern analysis as a tool for  
1034 constraining the interaction between regional and diapir-related stress field: Poza de  
1035 la Sal Diapir (Basque Pyrenees, Spain). In: *Salt Tectonics, Sediments and*  
1036 *Prospectivity*. Alsop, G.I., Archer, S.G., Hartley, A.J., Grant, N.T., Hodgkinson, R.  
1037 (eds). *Geological Society of London Special Publications* **363**, 521-532.
- 1038 Quintà, A., Tavani, S. 2012. The foreland deformation in the south-western Basque-  
1039 Cantabrian Belt (Spain). *Tectonophysics*. **576-577**. 4-19. DOI:  
1040 10.1016/j.tecto.2012.02.015.
- 1041 Quintana, L. 2012. Extensión e inversión tectónica en el sector central de la región  
1042 Vasco-Cantábrica (Cantabria, Vizcaya, norte de España). PhD Thesis. Universidad  
1043 de Oviedo, Oviedo. Spain. 560pp.
- 1044 Ramírez del Pozo, J. 191. Bioestratigrafía y Microfacies del Jurásico y Cretácico del  
1045 Norte de España (Región Cantábrica). *Memorias Instituto Geológico y Minero de*  
1046 *España* **78**, 1-357.
- 1047 Riba, O. and Juado, M. J. 1992. Reflexiones sobre la geología de la parte occidental de  
1048 la Depresión del Ebro. *Acta Geologica Hispanica*, **27**, 177-193.
- 1049 Robles, S., Pujalte, V., Valles, J.C. 1989. Sistemas sedimentarios del Jurásico de la  
1050 parte occidental de la Cuenca Vasco-Cantatábrica. *Cuadernos Geología Ibérica*. **13**,  
1051 185-198.
- 1052 Robles, S., Quesada, S., Rosales, I., Aurell, M., García-Ramos, J.C. 2004. El Jurásico  
1053 marino de la Cordillera Cantábrica. In: Vera, J.A. (ed.) *Geología de España*. SGE  
1054 IGME, Madrid, 279-285.
- 1055 Roca, E., Muñoz, J.A., Ferrer, O., Ellouz, N. 2011. The role of the Bay of Biscay  
1056 Mesozoic extensional structure in the configuration of the Pyrenean orogen:  
1057 Constraints from the MARCONI deep seismic reflection survey. *Tectonics*. **30**.  
1058 TC2001. doi: 10.1029/2010TC002735.

- 1059 Rodríguez Cañas, C., Hernáiz, P.P., Malagón, J., Serrano, A. 1994. Notas sobre la  
1060 estructura cabalgante de Rojas-Santa Casilda. *Geogaceta* **15**, 135-138.
- 1061 Rowan, M.G., Jackson, M.P.A., Trudgill, B.D. 1999. Salt-Related fault families and  
1062 fault welds in the Northern Gulf of Mexico. *AAPG Bulletin*, **83**, 1454-1484.
- 1063 Rowan, M.G., Peel, F.J., Vendeville, B.C. 2004. Gravity-driven Fold Belts on passive  
1064 Margins. In: McClay (eds). Thrust tectonics and hydrocarbon systems. *AAPG*  
1065 *Memoir*, **82**, 157-182.
- 1066 Rowan, M. 2014. Passive-margin salt basins: hyperextension, evaporite depositioon,  
1067 and salt tectonics. *Basin Research*, **26**, 154-182. DOI: 10.1111/bre.12043.
- 1068 Ruiz, M. 2007. Caracterització estructural i sismotectònica de la litosfera en el Domini  
1069 Pirenaico-Cantàbric a partir de mètodes de sísmica activa i passiva, Ph.D. thesis,  
1070 Univ. Barcelona, Barcelona, Spain.
- 1071 Salas, R., Guimerà, J., Mas, R., Martín-Closas, C., Meléndez, A., Alonso, Á. 2001.  
1072 Evolution of the Mesozoic Central Iberian Rift System and its Cainozoic inversion  
1073 (Iberian Chain). In: Ziegler, P.A., Cavazza, W., Robertson, A.H.F., Crasquin-Soleau,  
1074 S. (eds). *Peri-Tethys Memoir 6: Peri-Tethyan Rift/Wrench Basins and PASSive*  
1075 *Margins. Mémoires du Muséum National de l'Historie Naturelle*, **186**, 145-185.
- 1076 Schröder, B. 1987. Inversion tectonics along the western margin of the Bohemian  
1077 Massif. *Tectonophysics*, **137**, 93-100.
- 1078 Sepehr, M., Cosgrove, J., Moieni, M. 2006. The impact of cover rock rheology on the  
1079 style of folding in the Zagros fold-thrust belt. *Tectonophysics*, **429**, 265-281. DOI:  
1080 10.1016/j.tecto.2006.05.021.
- 1081 Sepher, M., Cosgrove, J.W. 2005. The role of the Kazerun fault zone in the formation  
1082 and deformation of the Zagros fold-thrust belt, Iran. *Tectonics*. **28**. TC5005.
- 1083 Serrano, A., Martínez del Olmo, W. 2004. Estructuras diapíricas de la zona meridional  
1084 de la Cuenca Vasco-Cantábrica. In: Vera, J.A. (Ed.), *Geología de España*. SGE-  
1085 IGME Madrid, pp. 334–338.
- 1086 Serrano, A., Hernáiz, P.P., Magalón, J. Rodríguez-Cañas, C. 1994. Tectónica distensiva  
1087 y halocinesis en el margen SO de la cuenca Vasco-Cantábrica. *Geogaceta*. **15**. 131-  
1088 134.
- 1089 Soto, R., Casas, A.M., Storti, F., Faccenna, C. 2002. Role of lateral thickness variations  
1090 on the development of oblique structures at the Western end of the South Pyrenean  
1091 Central Unit. *Tectonophysics*, **35**, 215-235.
- 1092 Spratt, D.A., Dixon, J.M., Beattie, E.T. 2004. Changes in structural style controlled by  
1093 lithofacies contrast across transverse carbonate bank margins - Canadian Rocky  
1094 Mountains and scaled physical models. In: McClay, K.R. (Ed.), *Thrust tectonic and*  
1095 *hydrocarbon systems: AAPG Memoir*, **82**, 259-275.

- 1096 Steward, S.A., Argent, J.D. 2000. Relationship between polarity of extensional fault  
1097 arrays and presence of detachments. *Journal of Structural Geology*. **22**, 693-711.
- 1098 Steward, S.A., Ruffell, A.H., Harvey, M.J. 1997. Relationship between basement-linked  
1099 and gravity-driven faults systems in the UKCS salt basins. *Marine and Petroleum*  
1100 *Geology*, **14**, 581-604.
- 1101 Tavani, S., Muñoz, J.A. 2012. Mesozoic rifting in the Basque-Cantabrian Basin (Spain):  
1102 Inherited faults, transversal structures and stress perturbation. *Terranova*. **24**, 70-76.  
1103 DOI: 10.1111/j.1365-3121.2011.01040.x.
- 1104 Tavani, S., Quintà, A., Granado, P. 2011. Cenozoic right-lateral wrench tectonics in the  
1105 Western Pyrenees (Spain): The Ubierna Fault System. *Tectonophysics*, **509**, 238-253.  
1106 DOI: 10.1016/j.tecto.2011.06.013.
- 1107 Tavani, S.; Carola, E.; Granado, P.; Quintà, A.; Muñoz, J.A. 2013. Transpressive  
1108 inversion of a Mesozoic extensional forced fold system with an intermediate  
1109 décollement level in the Basque-Cantabrian Basin (Spain). *Tectonics* v32.  
1110 DOI:10.1002/tect.20019.
- 1111 Veen, V. 1965. The tectonic and stratigraphic history of the Cardaño area, Cantabrian  
1112 Mountains, northern Spain. *Leidsche Geol. Meded.* **35**, 45-104.
- 1113 Vendeville, B.C., Jackson, M.P.A. 1992. The rise of diapirs during thin-skinned  
1114 extension. *Marine and Petroleum Geology*. **9**, 331-353.
- 1115 Vergés, J., García-Senz, J. 2001., Mesozoic evolution and Cainozoic inversión of the  
1116 Pyrenean Rift, in *Peri-Tethys Memoir 6: Peri-Tethyan Rift/Wrench Basins and*  
1117 *Passive Margins*, edited by P. A. Ziegler et al., *Mém. Mus. National Hist. Nat.*, **186**,  
1118 187-212.
- 1119 Vergés, J., Fernández, M., Martínez, A., 2002. The Pyrenean origin: pre-, syn-, and  
1120 post-collisional evolution. In: Rosenbaum, G., Lister, G.S., (Eds.), *Reconstruction*  
1121 *of the Evolution of the Alpine-Himalayan Orogen*. *Journal of the Virtual Explorer*  
1122 **8**, 57-76.
- 1123 Vidal-Royo, O., Koyi, H.A., Muñoz, J.A. 2009. Formation of orogen-perpendicular  
1124 thrusts due to mechanical contrasts in the basal décollement in the Central External  
1125 Sierras (Southern Pyrenees, Spain). *Journal of Structural Geology* **31**, 523-539.
- 1126 Wagner, R.H., Winkler Prins, C.F., Riding, R.E., Wagner-Gentis, C.H.T. 1971.  
1127 Lithostratigraphic units of the lower part of the Carboniferous in northern León,  
1128 Spain. *Trabajos de Geología* **4**, 603-663.
- 1129 Whithjack, M.O., Callaway, S. 2000. Active normal faulting beneath a salt layer: An  
1130 experimental study of deformation patterns in the Cove Sequence. *American*  
1131 *Association of Petroleum Geologists Bulletin*. **84**, 627-651.

1132 Ziegler, P.A. (Ed.), 1987. Compressional Intra-Plate Deformation in the Alpine  
1133 Foreland. *Tectonophysics*, vol. 137, 420 pp.

1134 **9 Figure caption**

1135 Figure 1: A) Elevation map of the W-E Pyrenean Orogen and surroundings with the  
1136 major domains labelled. STZ and PTZ corresponds to Santander and Pamplona Transfer  
1137 Zones respectively. B and C) S-N cross-sections of the Cantabrian Mountains and the  
1138 Basque-Pyrenees (Modified from Pulgar *et al.*, 1999; Riba and Jurado, 1992). D)  
1139 Schematic S-N models purposed by different authors in order to explain the main  
1140 features and the deformation style of the Burgalesa Platform Domain and adjacent  
1141 areas.

1142

1143 Figure 2: Cronostratigraphic column of the study area with the main tectonic events that  
1144 took place. (Partially modified from Barnolas and Pujalte, 2004).

1145

1146 Figure 3: Geological map of the Burgalesa Platform and surroundings with the location  
1147 of the different seismic lines, wells and cross-sections shown in this work as well as the  
1148 foreland deformation interpreted from the seismic sections.

1149

1150 Figure 4: S-N seismic section of the Duero Foreland Basin and the eastern part of the  
1151 Cantabrian Mountains with thrusts affecting the Cenozoic succession as well as the  
1152 Mesozoic and the basement. See figure 3 for location.

1153

1154 Figure 5: W-E seismic section showing the involvement of the basement in the western  
1155 sector of the Burgalesa Platform producing the plunge observable in the Mesozoic  
1156 succession at surface. See figure 3 for location.

1157

1158 Figure 6: S-N seismic sections located in the Huidobro area where the Tejón Profundo-1  
1159 well testifies a repetition of the Mesozoic succession and how this back-thrust is imaged  
1160 in the lines. Note how the structural relief decreases westwards. See figure 3 for  
1161 location.

1162

1163 Figure 7: W-E seismic section in the Villalta area showing the hangingwall cutoff of the  
1164 back-thrust present in this sector of the Burgalesa Platform. The deeper reflectors show  
1165 the transversal extensional fault delimiting the former Basque-Cantabrian Basin and  
1166 how during the inversion of the basin, the Mesozoic succession was south-eastwards  
1167 displaced favoured by the presence of the Upper Triassic salts acting as a detachment  
1168 level. See figure 3 for location.

1169

1170 Figure 8: Composed W-E and SW-NE seismic section in the Bureba sub-basin  
1171 reflecting the eastward thinning of the Lower Cretaceous succession related to the  
1172 extensional event that produced forced folding of the Jurassic units. The contractional  
1173 structure, displacing the Mesozoic succession towards the SE, is fossilised by the  
1174 Cenozoic sediments of the Bureba and the Ebro Foreland Basin. See figure 3 for  
1175 location.

1176

1177 Figure 9: W-E seismic section of the Bureba re-entrant displaying flat-lying Mesozoic  
1178 and Cenozoic successions and S-N seismic section of the western part of the Basque-  
1179 Pyrenees with the Mesozoic and Cenozoic succession southward displaced by a thrust  
1180 detached at the Upper Triassic salt that overrides the Ebro Foreland Basin.

1181

1182 Figure 10: Cross-sections of the study area. Three in a S-N orientation and one in a  
1183 NW-SE with both, the main areas and wells labelled. See figure 3 for location.

1184

1185 Figure 11: Schematic map with the distribution of the salt thickened areas and the  
1186 location of the syn-rift depocenters and thinned parts and also the location of some of  
1187 the wells of the study area.

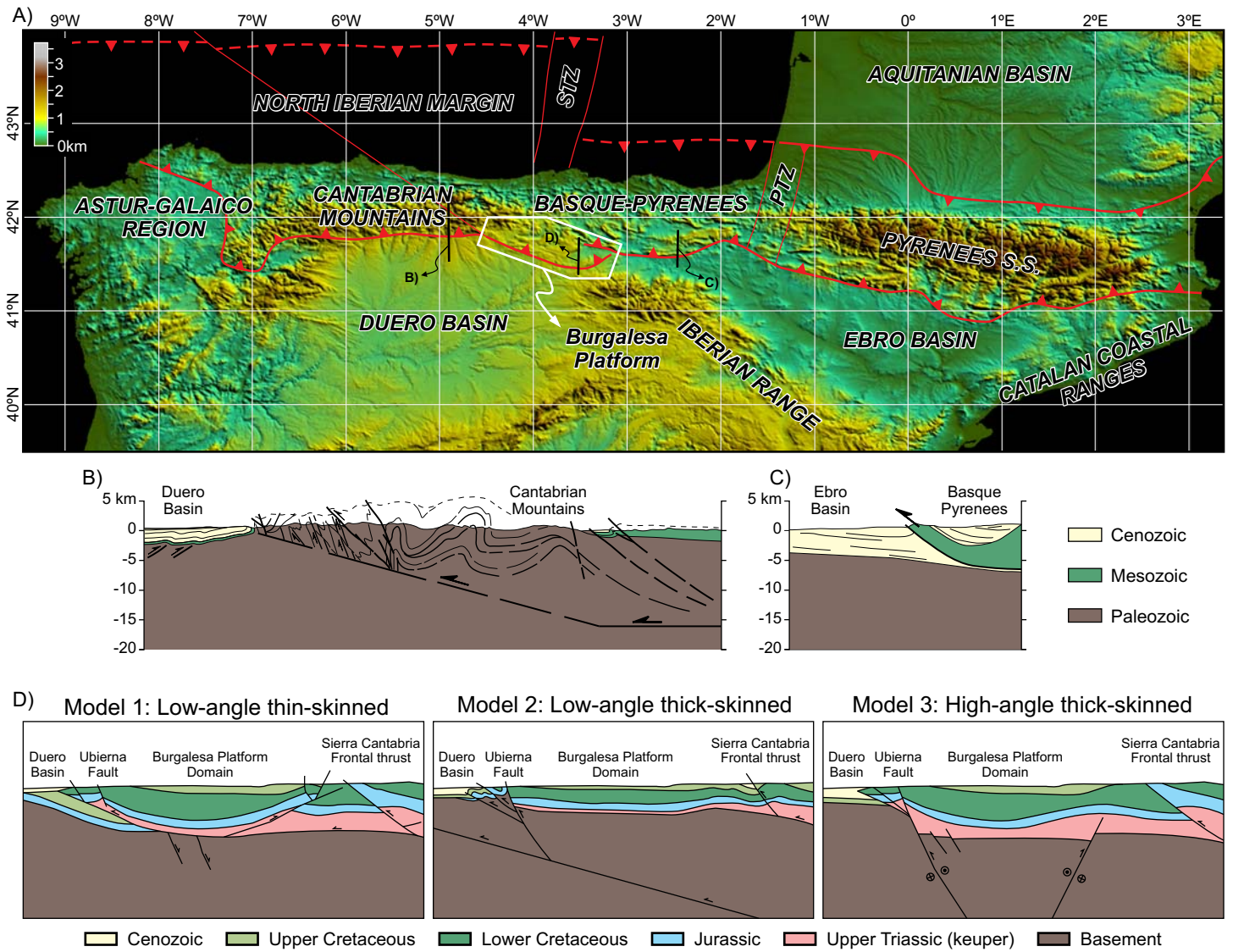
1188

1189 Figure 12: A) Geological map with the distribution of the onlap geometries observed in  
1190 the seismic sections. Red arrows indicate the direction of migration of the onlaps. B) S-  
1191 N seismic section crossing the Folded Band and the Burgalesa Platform highlighting the  
1192 onlaps.

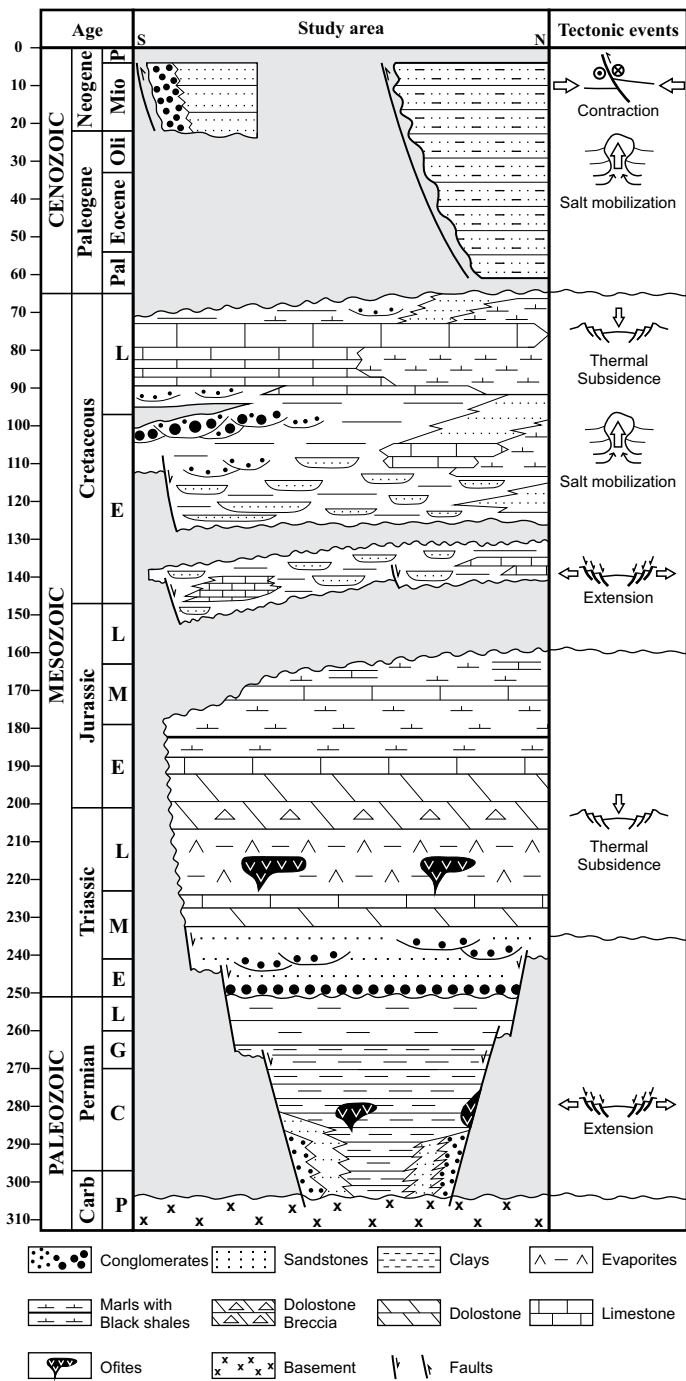
1193

1194 Figure 13: Map of the study area and surrounding with the movement directions of each  
1195 area and also the main domains (i.e. Thick-skinned, Thin-skinned and Autochthonous)  
1196 described in the text and present in the area. UCAFC corresponds to Upper Cretaceous  
1197 Autochthonous Footwall Cutoff.

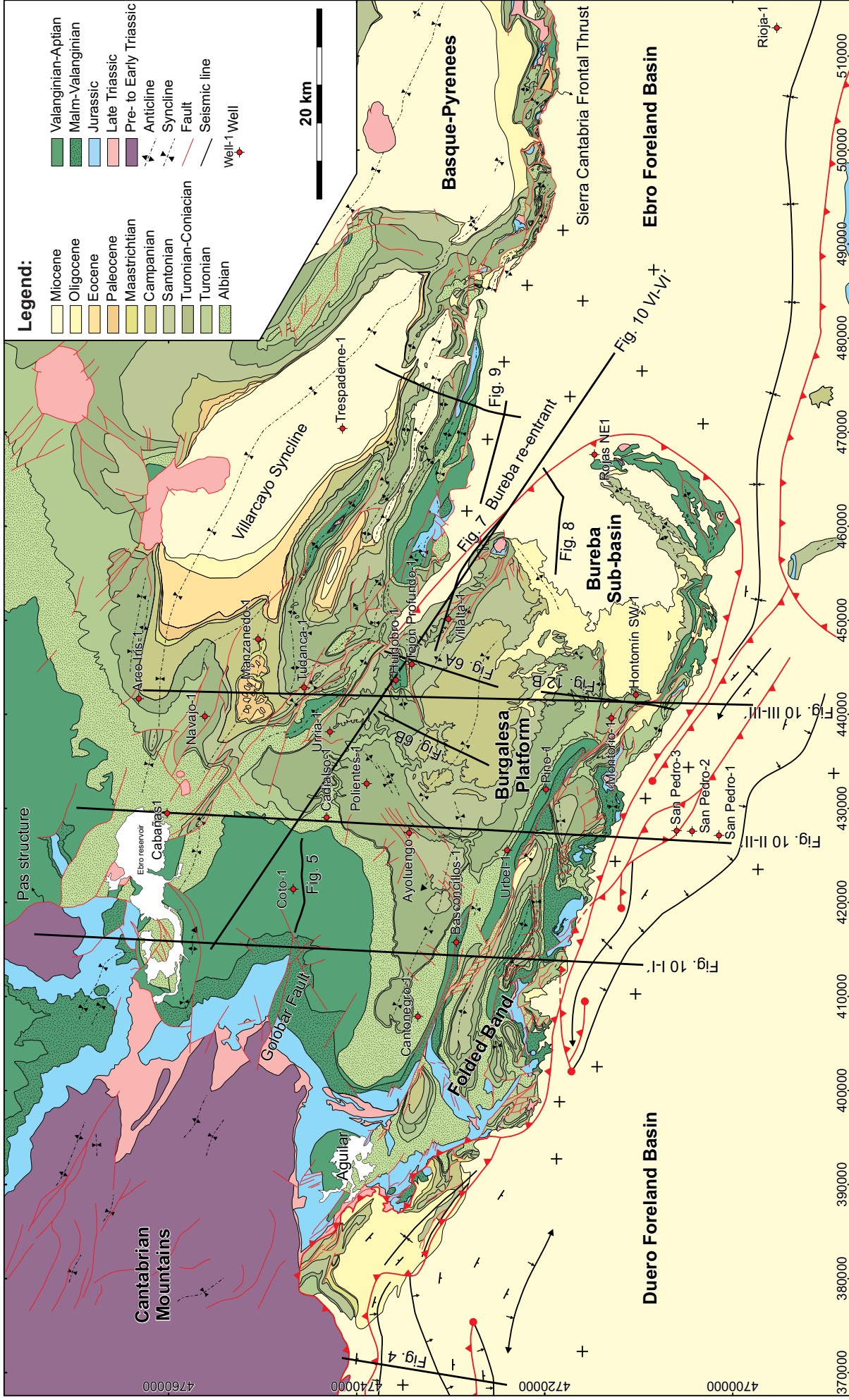
1198



**Fig. 1 (double column)**

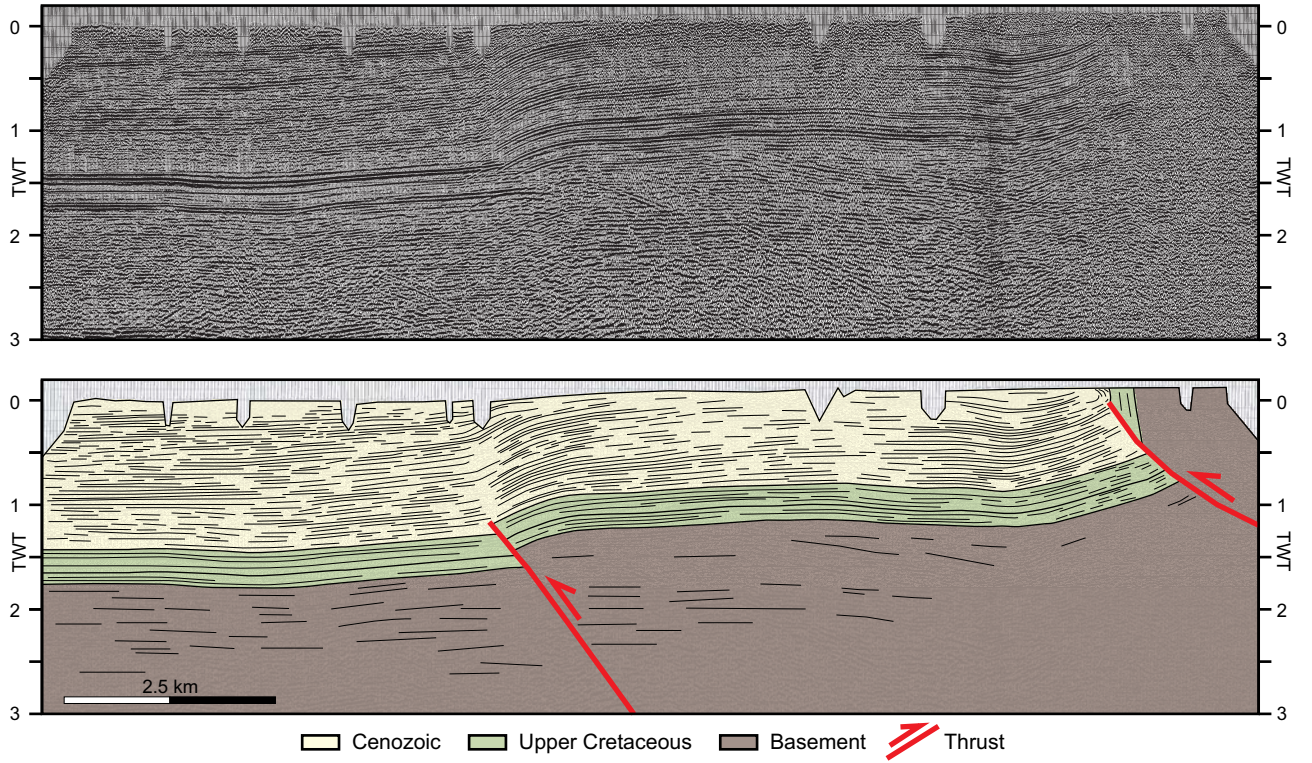


**Fig. 2 (single column)**

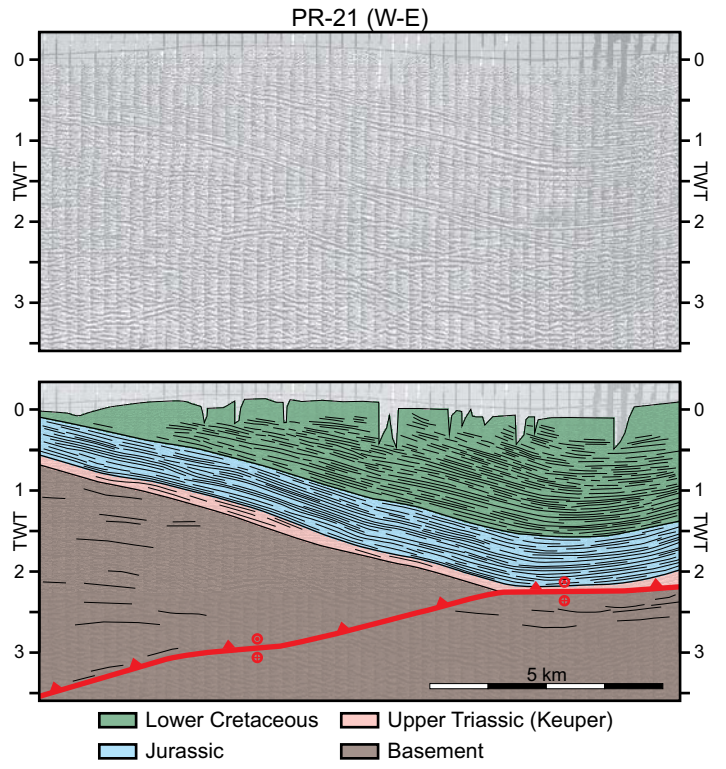


**Fig. 3 (double column)**

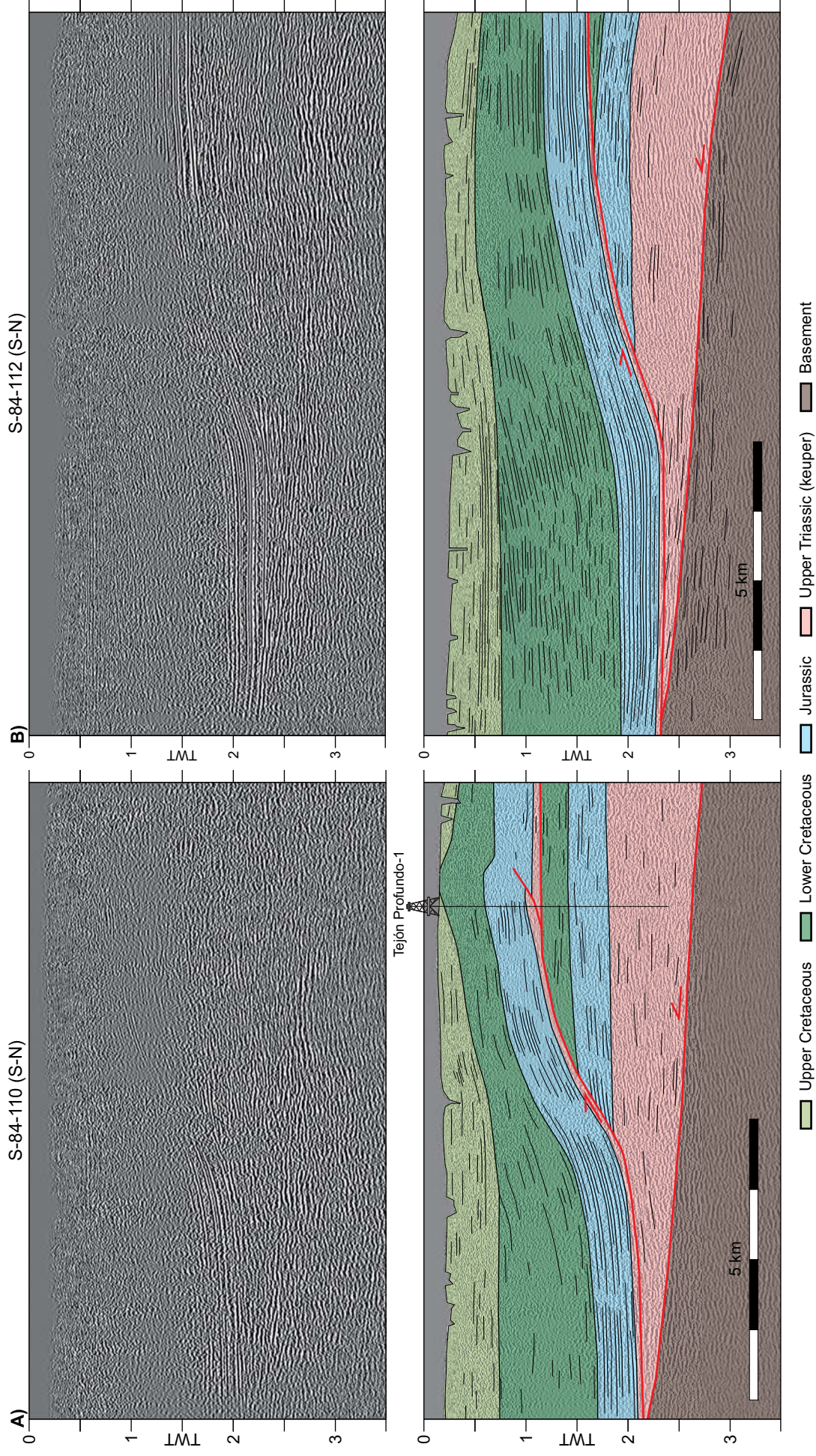
DR-85-02 (S-N)



**Fig. 4 (double column)**

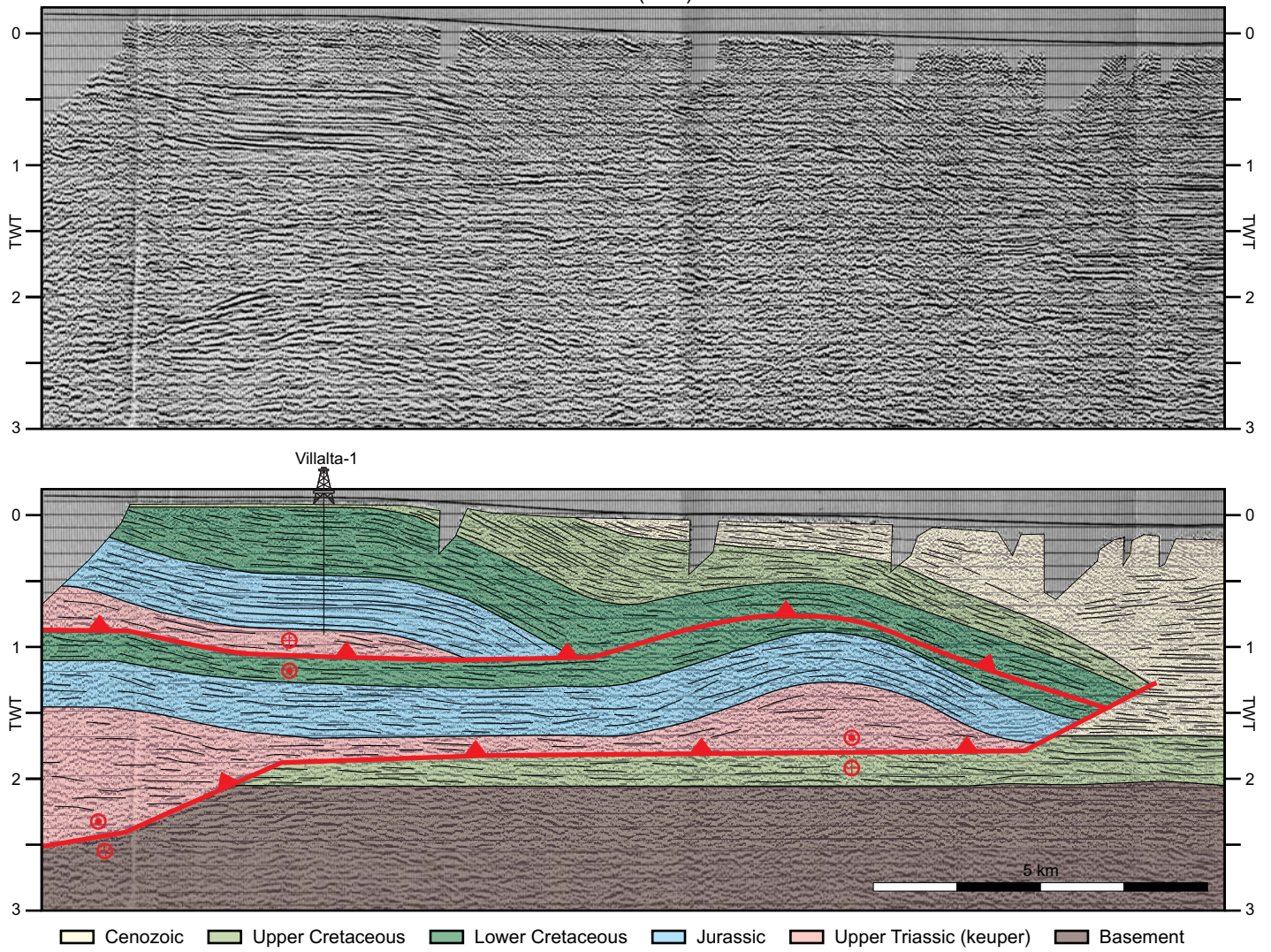


**Fig. 5 (single column)**

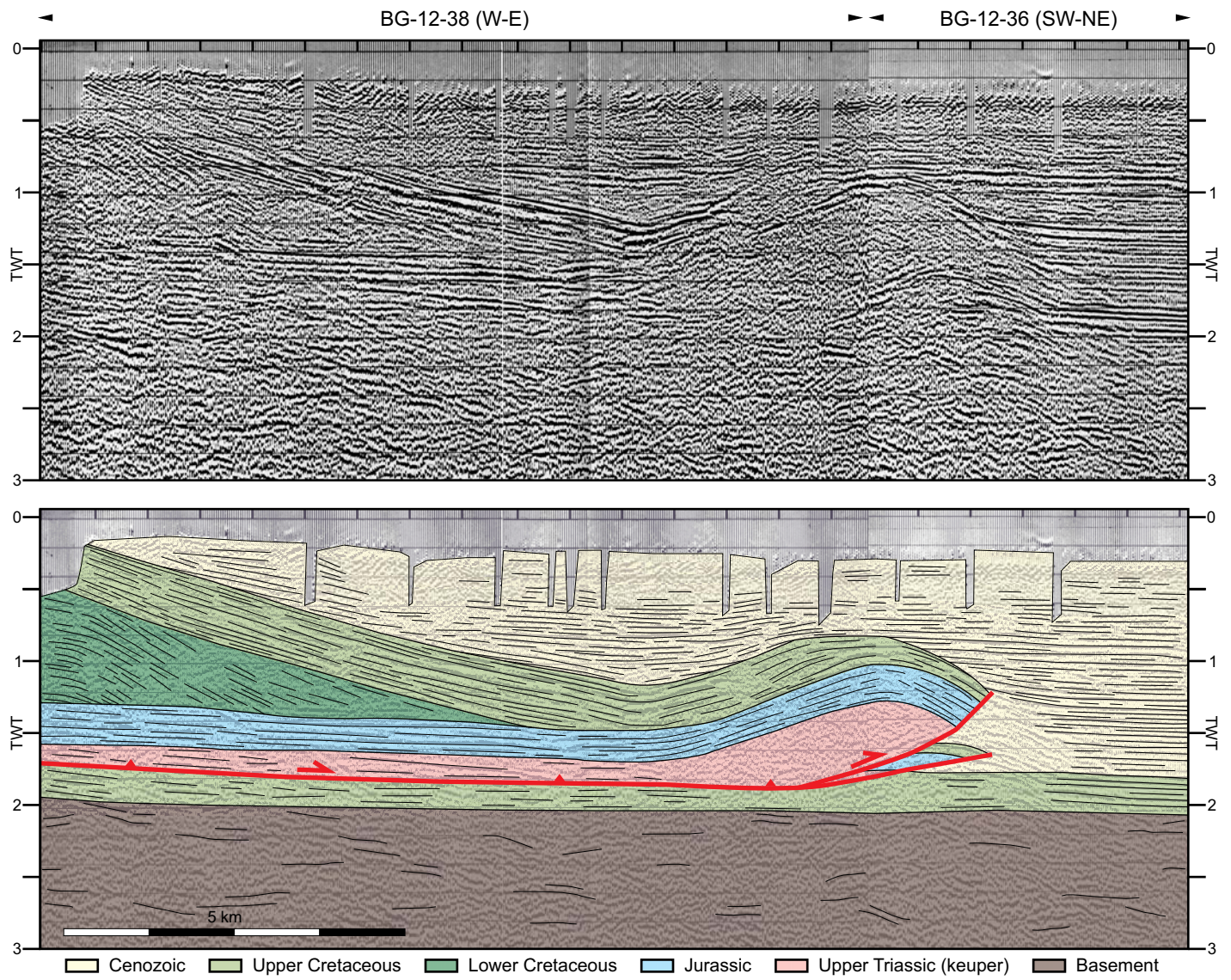


**Fig. 6(double column)**

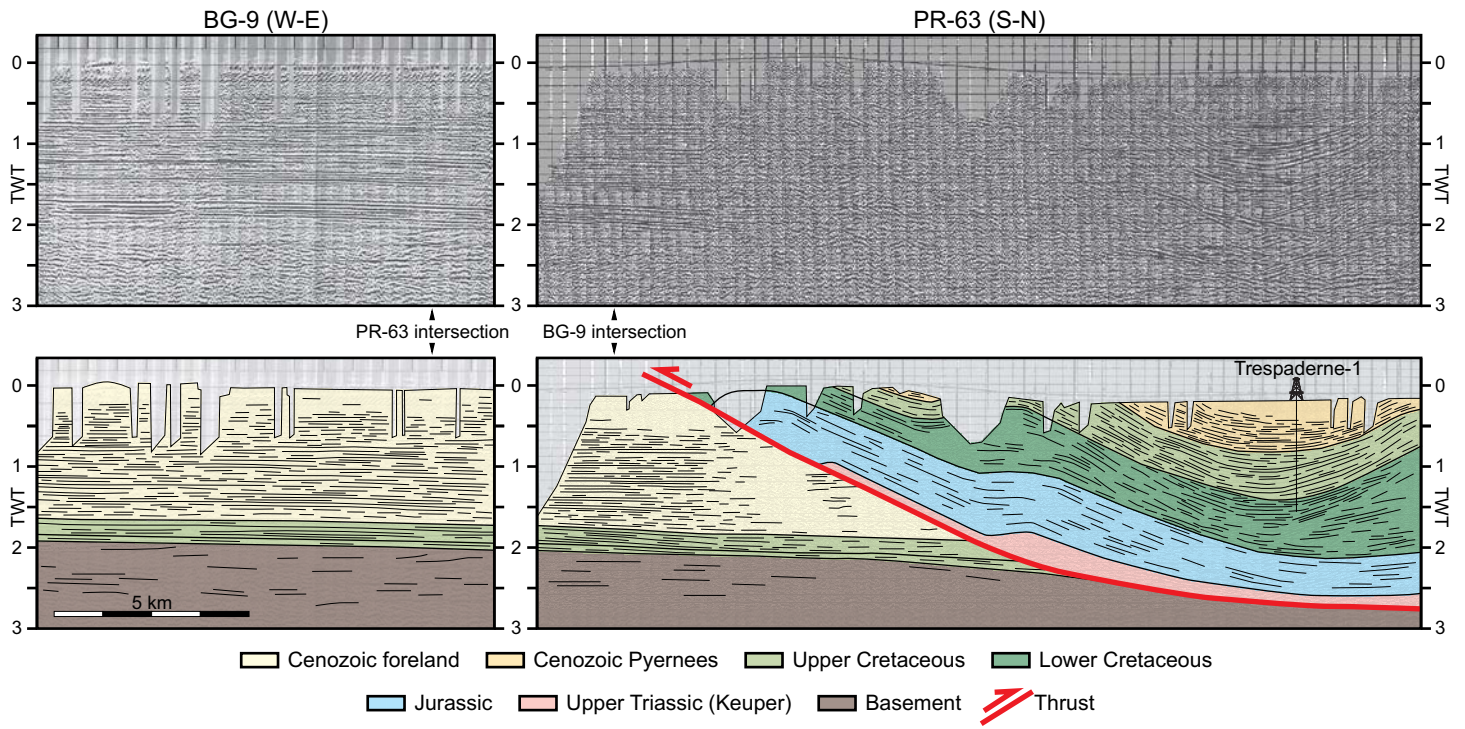
VAL-1 (W-E)



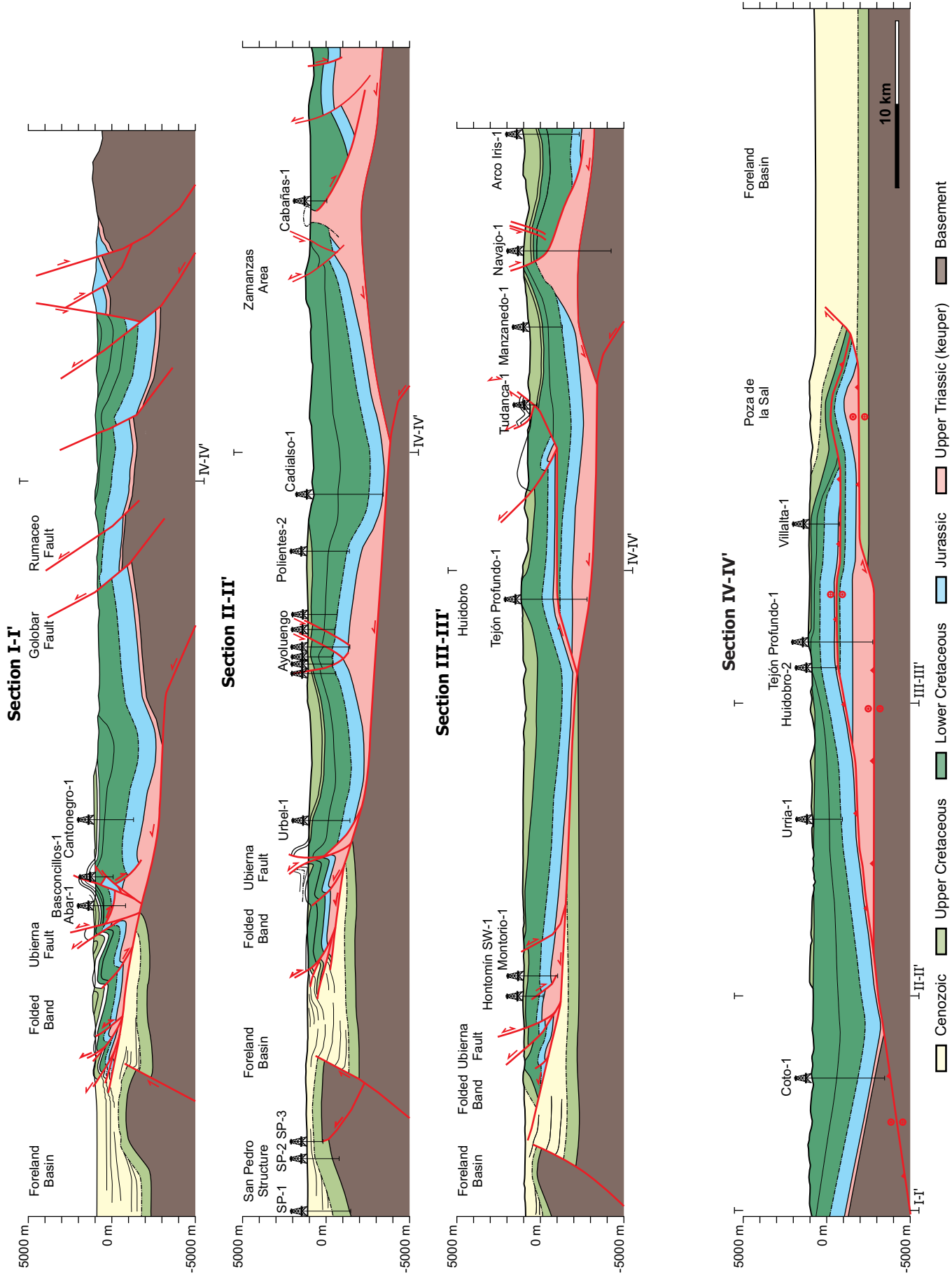
**Fig. 7 (double column)**



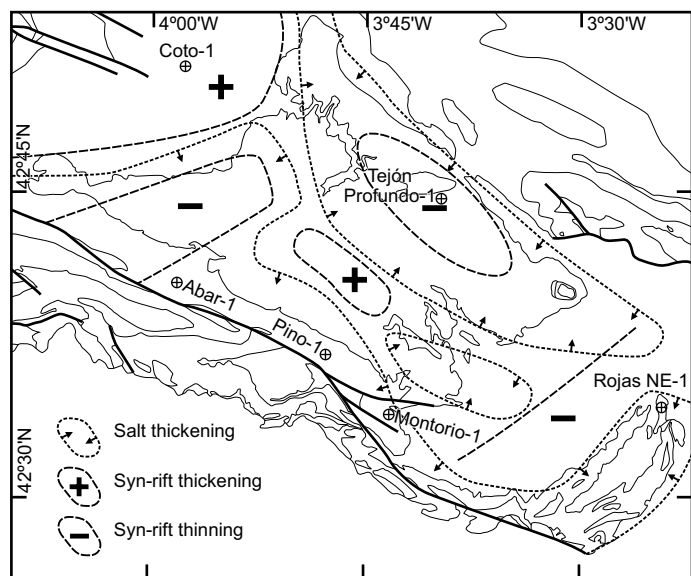
**Fig. 8 (double column)**



**Fig. 9 (double column)**

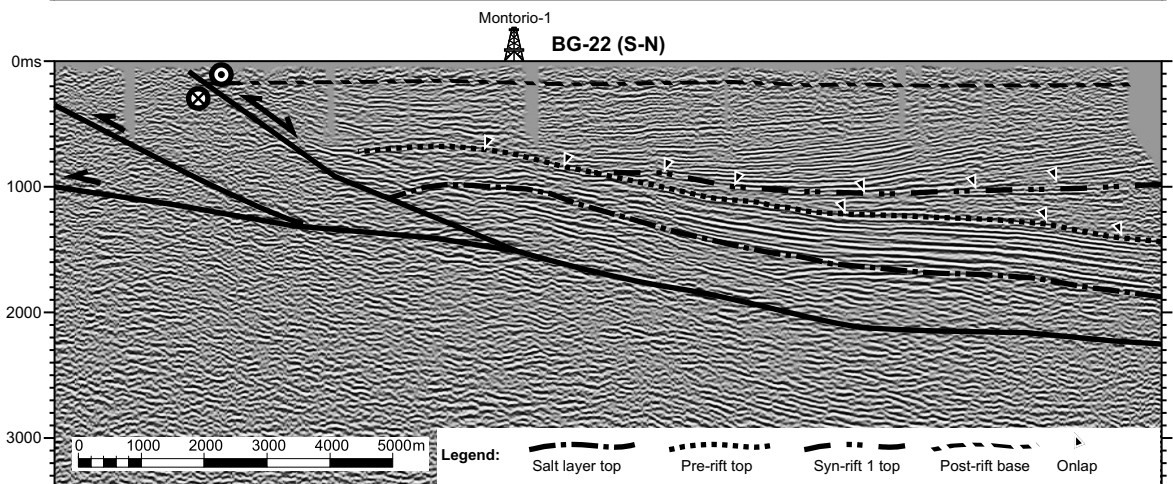
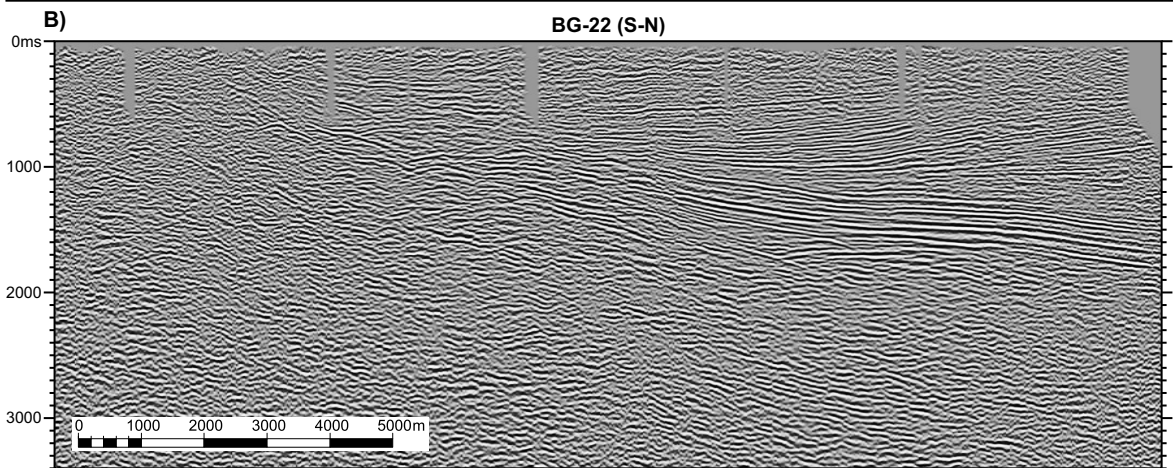
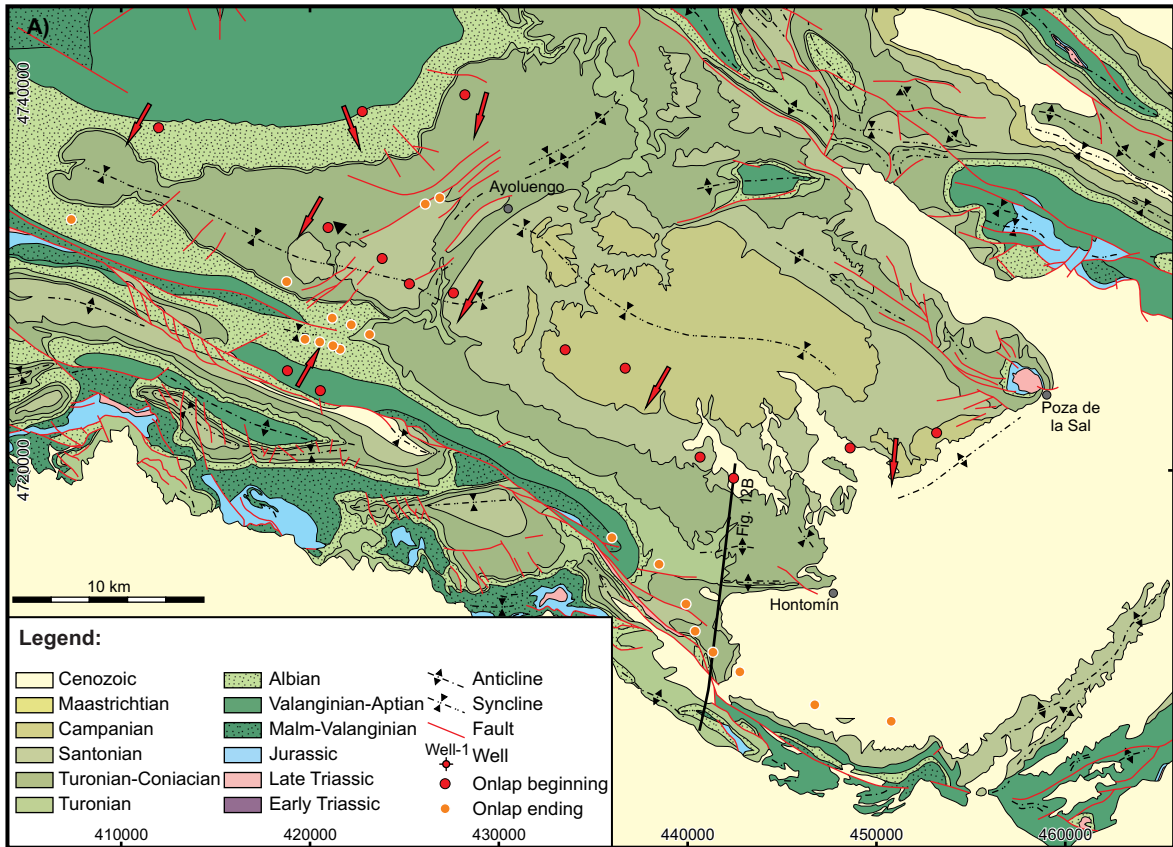


**Fig. 10 (double column)**



**Fig. 11 (single column)**

# Fig. 12 (double column)



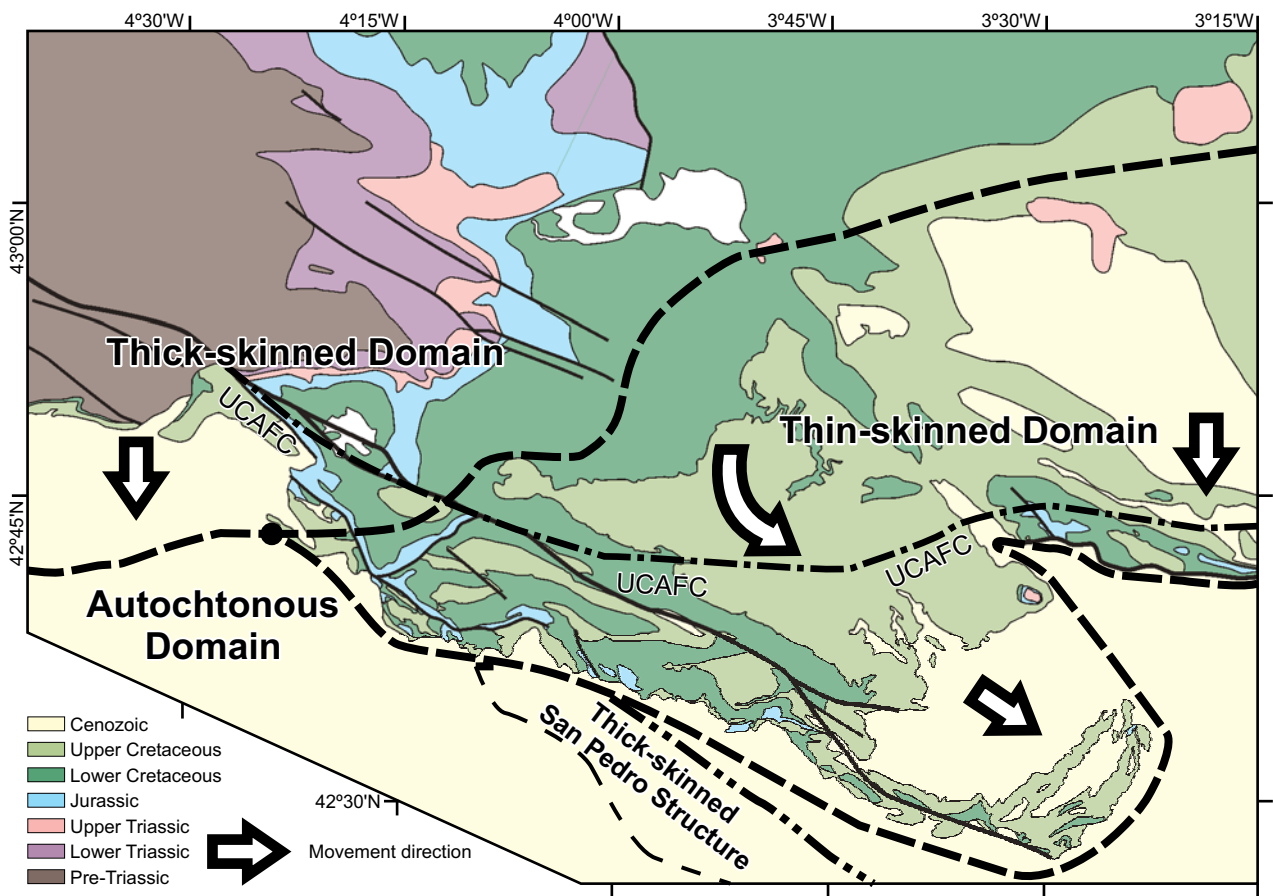


**Fig. 13 (double column)**